

## Review

CO<sub>2</sub> Gas hydrate for carbon capture and storage applications – Part 1

Morteza Aminnaji <sup>a,b,c,\*</sup>, M Fahed Qureshi <sup>d</sup>, Hossein Dashti <sup>e,f</sup>, Alfred Hase <sup>b</sup>, Abdolali Mosalanejad <sup>g</sup>, Amir Jahanbakhsh <sup>h,i,\*\*</sup>, Masoud Babaei <sup>c</sup>, Amirpiran Amiri <sup>j</sup>, Mercedes Maroto-Valer <sup>h,i</sup>

<sup>a</sup> Institute of GeoEnergy Engineering, Heriot-Watt University, Edinburgh, EH14 4AS, UK

<sup>b</sup> ChampionX, Bunderbank Technology Centre, Peterseat Drive, Aberdeen, AB12 3HT, UK

<sup>c</sup> Department of Chemical Engineering and Analytical Science, University of Manchester, Manchester, M13 9PL, UK

<sup>d</sup> Department of Chemical and Biomolecular Engineering, National University of Singapore, Singapore, 117580

<sup>e</sup> APA Group, 80 Ann St, Brisbane, QLD 4000, Australia

<sup>f</sup> School of Chemical Engineering, The University of Queensland, Brisbane, QLD 4072, Australia

<sup>g</sup> Department of Petroleum Engineering, School of Chemical and Petroleum Engineering, Shiraz University, Shiraz, Iran

<sup>h</sup> The Research Centre for Carbon Solutions (RCCS), School of Engineering and Physical Sciences, Heriot-Watt University, Edinburgh, UK

<sup>i</sup> Industrial Decarbonisation Research and Innovation Centre (IDRIC), Heriot-Watt University, Edinburgh, UK

<sup>j</sup> Energy and Bioproducts Research Institute (EBRI), College of Engineering and Applied Science, Aston University, UK

## ARTICLE INFO

Handling Editor: Ruzhu Wang

## ABSTRACT

Gas hydrates are solid crystalline compounds formed by water and gas molecules through molecular interactions, typically at low temperatures and high pressures. While gas hydrates are generally known as flow assurance challenges for the oil and gas industries (e.g., pipeline blockages), numerous studies have shown the potential application of gas hydrate in carbon capture and storage (CCS).

Due to the more thermodynamic stability of CO<sub>2</sub> hydrate compared to other industrial emission gas components like nitrogen, CO<sub>2</sub> hydrates have emerged as a viable mechanism for CO<sub>2</sub> capture. Moreover, a large volume of CO<sub>2</sub> can be stored securely in the stable structure of gas hydrates, providing an additional benefit for CO<sub>2</sub> storage in geological formations. Thus, gas hydrates can be suggested as a technology for mitigating CO<sub>2</sub> emissions.

Notwithstanding the CO<sub>2</sub> hydrate advantages in CCS, they may also present some challenges, particularly in terms of flow assurance. For example, CO<sub>2</sub> hydrate formation during CO<sub>2</sub> transportation can cause a serious pipeline blockage. Therefore, the fundamental understanding of gas hydrates is crucial for CCS. In the first part of this review, the principle on gas hydrates (especially CO<sub>2</sub> hydrates) and CO<sub>2</sub> hydrate-based carbon capture are discussed.

## 1. Introduction

Gas hydrates are solid crystalline compounds that contain water molecules and suitably sized guest molecules. Clathrate hydrates form through the physical combination of water and guest molecules under certain pressure and temperature conditions (i.e., typically low temperatures and elevated pressures). The water molecules form cages through hydrogen bonding (an attractive interaction of a hydrogen atom with an electronegative atom such as oxygen) and trap guest molecules. The guest molecules can rotate inside the cavities as there is no bonding

between water and guest molecules. In contrast to inorganic hydrates (e.g., CaCl<sub>2</sub>·6H<sub>2</sub>O), gas hydrates are non-stoichiometric crystalline compounds with different hydration numbers (i.e., hydration number is the mole fraction ratio of water to guest molecules).

The gas hydrate flow assurance-related area was the principal hydrate research to prevent or minimise the risk of hydrate blockage in the pipeline. However, due to its unique advantages, gas hydrate is now considered for various applications, such as gas storage (i.e., high gas storage capacity), seawater desalination, carbonated solid foods, refrigeration, gas separation, energy production from hydrate

\* Corresponding author. Institute of GeoEnergy Engineering, Heriot-Watt University, Edinburgh, EH14 4AS, UK

\*\* Corresponding author. The Research Centre for Carbon Solutions (RCCS), School of Engineering and Physical Sciences, Heriot-Watt University, Edinburgh, UK

E-mail addresses: [morteza.aminaji@championx.com](mailto:morteza.aminaji@championx.com) (M. Aminnaji), [a.jahanbakhsh@hw.ac.uk](mailto:a.jahanbakhsh@hw.ac.uk) (A. Jahanbakhsh).

reservoirs, etc. Certainly, the application of CO<sub>2</sub> hydrate can be utilised for CO<sub>2</sub> capture and storage applications through carbon capture and storage (CCS) process to promote sustainable economic growth. The simple procedure of CO<sub>2</sub> capture using hydrate makes it sustainable technology compared to other traditional technologies. Furthermore, CO<sub>2</sub> gas hydrate can be exploited for permanent storage of CO<sub>2</sub> in geological formations through CH<sub>4</sub>-CO<sub>2</sub> replacement in the permafrost gas hydrate reservoir. Notwithstanding the importance of CO<sub>2</sub> hydrate application for CO<sub>2</sub> capture and storage, there is still a challenge to reduce the risk of CO<sub>2</sub> hydrate formation during transportation (i.e., CO<sub>2</sub> is normally captured from the large point sources and transported via pipelines or ship to store in a safe place).

This review paper includes two parts which provides a fundamental understanding of advances in gas hydrates chemistry and technologies that are potentially applicable and relevant in CCS. Due to the global attention and interest in CCS, the research, advances, and developments in sustainable hydrate-based technologies are growing fast. Therefore, this review focuses on hydrate-based technologies particularly relevant for CCS.

**Fig. 1** shows the graphical content for the sections and topics that are covered in both part 1 and part 2. In Part 1, the importance of carbon management and sequestration is firstly discussed. Part 1 then aims to review the gas hydrate chemistry and properties (focused on CO<sub>2</sub> hydrate). Carbon capture is the first stage in the CCS chain. Therefore, the last section of part 1 provides a fundamental understanding of the most recent advances and research in hydrate-based carbon capture technologies.

## 2. Importance of carbon management

One of the essential biochemical cycles for sustaining life on Earth is carbon cycle. Carbon is the main component that exchanges among the biosphere, hydrosphere, geosphere, pedosphere, and atmosphere (**Fig. 2**). The long-term process of carbon movement, as well as carbon sequestration to the carbon sinks, can be described by the carbon cycle [1]. About one-quarter of the carbon released by human activities sinks into the land and ocean each year [2]. The excessive carbon emissions caused by human activities, such as modifying land use and mining fossil carbon from the geosphere, have disrupted the biological carbon cycle

[1,3].

The two main forms of carbon in the atmosphere are carbon dioxide and methane. These gases are highly effective at trapping heat in the atmosphere, leading to global warming [4]. Compared to carbon dioxide, methane has a stronger greenhouse effect per unit of volume. However, methane is more short-lived than carbon dioxide, and its concentration in the atmosphere is much lower. Therefore, the impact of carbon dioxide as greenhouse effect is more significant [5].

Since the Industrial Revolution began in 1760, the atmospheric concentration of CO<sub>2</sub> and other greenhouse gases has been rising exponentially and has now reached a critical level [6–8]. According to studies from the International Energy Outlook, worldwide energy consumption was approximately 549 quadrillion Btu in 2012 and is predicted to continue to rise to 815 quadrillion Btu in 2040, an increase of 48 % [9]. For the next several decades, fossil fuels will remain the cornerstone of global energy. It is essential to implement appropriate measures to control CO<sub>2</sub> emissions resulting from the combustion of fossil fuels for power generation [9,10].

Anthropogenic activities, such as cement and steel production, deforestation, and fossil-fuel combustion for power and transportation, have disrupted the natural equilibrium by adding excessive carbon dioxide to the atmosphere [11–13]. The level of carbon dioxide concentration in 2020 has increased by 52 % since the Industrial Revolution. As a consequence of increased carbon dioxide emissions, marine chemistry has been significantly altered due to carbon dioxide dissolution in the water, increasing the acidity of the ocean surface by 30 % [14–16]. Based on a NASA GIS study in 2019, the climate change model developed by the assessment of greenhouse gases (MAGICC) predicts that, if the current fossil fuel-intensive emission trajectory continues, the global average temperature rise will be greater than 4 °C by the end of the century [2].

The impacts of higher temperatures and consequently higher rates of evaporation can be summarized as more severe heat waves and drought, a higher risk of terrestrial vegetation destruction, possible lack of food supplies, ocean warming and acidification (with about 90 % of all heat and 25 % of carbon dioxide transferred into the ocean), and rising sea levels caused by the melting of North Sea ice [2,14,15].

The current concentration of carbon dioxide is approximately 410 ppm [2]. Various studies have shown that a target carbon dioxide

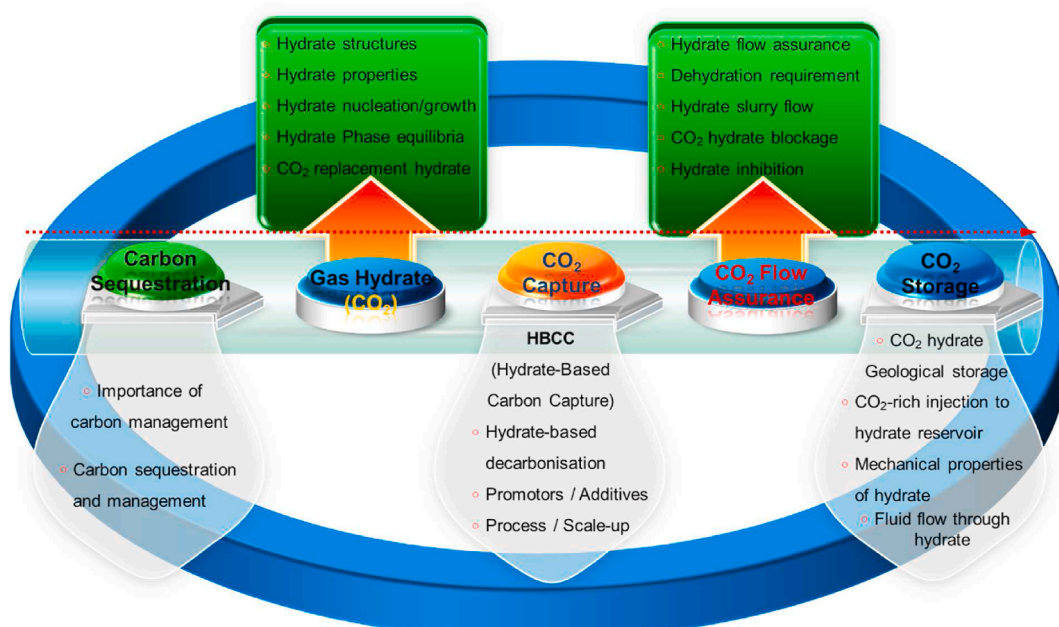


**Fig. 1.** A graphical representation summarizing the key concepts explored in this review.

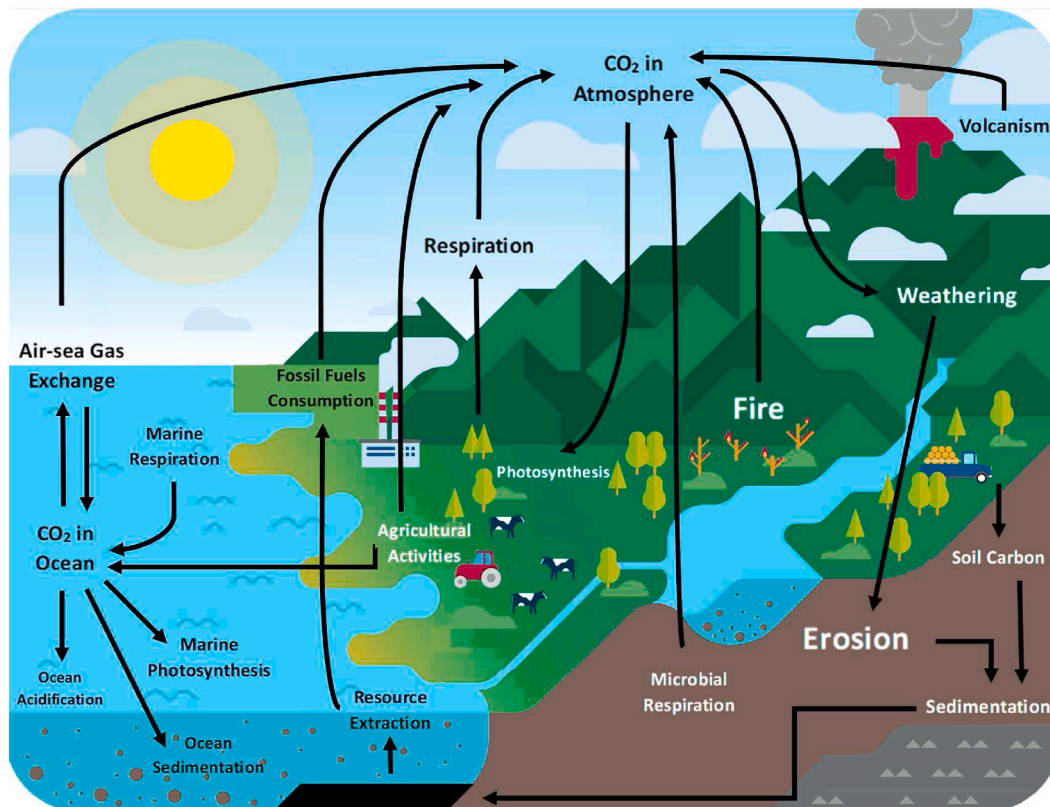


**Fig. 2.** The movement of carbon occurs among the atmosphere, hydrosphere, biosphere, and pedosphere over a range of timeframes, varying from hours to centuries.

concentration of 450 ppm is needed to stabilize the average global temperature rise at 2 °C by the end of 2100. It is estimated that between 40 % and 70 % of total carbon dioxide emissions must be reduced by 2050 to maintain the optimum carbon dioxide concentration [2,10,17]. Therefore, it is crucial to avoid any delays in executing countermeasures to manage carbon emissions. Note that, based on the current situation, CO<sub>2</sub> management can be defined as a procedure that seeks a cure rather than preventing the problem.

### 3. Gas hydrate

#### 3.1. Gas hydrate structures

Gas hydrates consist of various cages/cavities which are polyhedral described by nomenclature  $n_i m_i$  where  $n_i$  is the number of edges in polygon type  $i$  and  $m_i$  is the number of  $n_i$  type polygon. The combination of varying hydrate cavities results in the formation of various hydrate

structures. Canonical clathrate hydrates and semi-clathrate hydrates are the two main hydrate categories. While canonical clathrate hydrates do not have direct host-guest interaction, there are directional guest-host interactions in the semi-clathrate hydrates. They have many similar properties as described in the following sections.

##### 3.1.1. Clathrate hydrates

The guest molecules are not bonded to water molecules in the canonical clathrate hydrates. They can rotate through the van der Waals forces inside the hydrogen-bonded water lattice. Structure-I (sI), structure-II (sII), and structure-H (sH) are three main hydrate structures (Fig. 3). These structures consist of various cavities, including pentagonal dodecahedron ( $5^{12}$ ), tetrakaidecahedron ( $5^{1,2}6^2$ ), hexakaidecahedron ( $5^{1,2}6^4$ ), irregular dodecahedron ( $4^35^66^3$ ), and icosahedron ( $5^{1,2}6^8$ ), as shown in Fig. 4.

Structure-I hydrate is a cubic crystal structure with space group  $Pm\bar{3}n$  and forms from small molecules with size of 0.4–0.55 nm (e.g., C<sub>1</sub>,

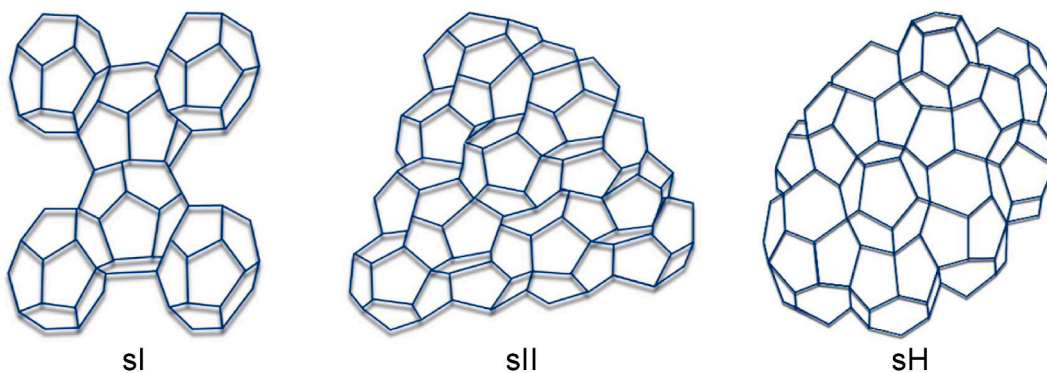


**Fig. 3.** Clathrate hydrate structures: Structure I (sI), Structure II (sII), and Structure H (sH). The structures are taken from Ref. [18].

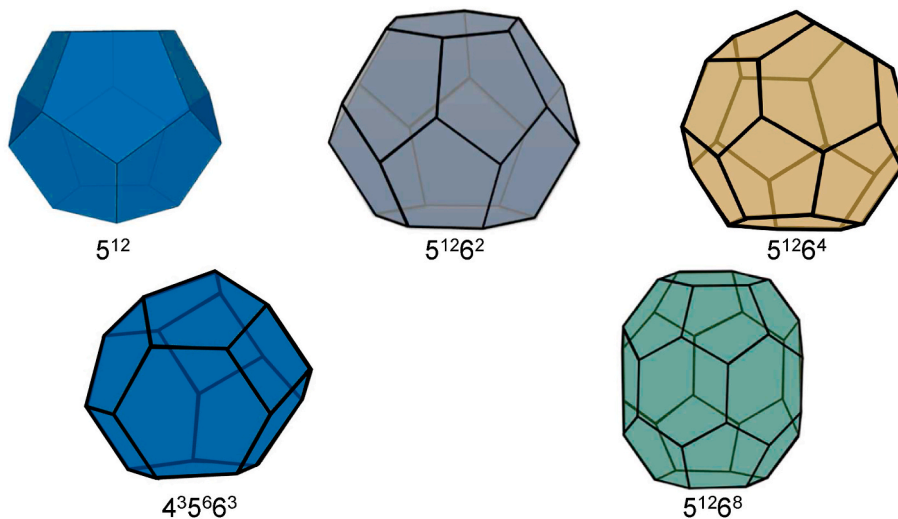


**Fig. 4.** Clathrate hydrate cavities: pentagonal dodecahedron ( $5^{12}$ ), tetrakaidecahedron ( $5^{1,2}6^2$ ), hexakaidecahedron ( $5^{1,2}6^4$ ), irregular dodecahedron ( $4^35,6^3$ ), and icosahedron ( $5^{1,2}6^8$ ).

$C_2$ ) [18,19]. Cubic sI with a unit cell size of  $12\text{ \AA}$  is composed of 46 water molecules forming six large cages ( $5^{1,2}6^2$ , comprising 12 pentagons and two hexagons) and two small cages ( $5^{12}$ , comprising 12 pentagons). In sI hydrates,  $5^{12}$  cavities join only through vertices without direct face sharing. The  $5^{12}$  cavities are placed in a position where they fill the space between each set of two  $5^{1,2}6^2$  cavities in a column [20,21].

The molecules with an intermediate size of 0.6–0.7 nm (e.g.,  $C_3$ ,  $C_4$ ) form sII hydrate in the form of cubic crystal structure with space group  $Fd3m$  [18,19]. Some small molecules (e.g.,  $N_2$  and  $O_2$ ) with a size of less than 0.4 nm can also form sII hydrates [18]. A unit cell of sII hydrates with a size of  $17.3\text{ \AA}$  is composed of 136 water molecules forming 16 small cages ( $5^{12}$ ) and eight large cages ( $5^{1,2}6^4$ ). In the cubic sII hydrate,  $5^{12}$  cavities share their faces in which  $5^{1,2}6^4$  are placed in empty spaces [20].

Structure-H (sH) with space group  $P6/mmm$  consists of 34 water molecules forming three small cages ( $5^{12}$ ), two medium cages ( $4^35,6^3$ ), and one large cage ( $5^{1,2}6^8$ ) [19]. While a single guest molecule can form stable sI and sII hydrates, two guest molecules (including one large guest molecule and one small guest molecule, e.g., methane + neohexane) are required to form a stable sH [22,23]. Larger guest molecules fill the large cage, and small guest molecules stabilize the two smaller cages of sH [24].

While some single guest molecules such as methane usually form sI, they can form sII (or even sH) hydrates under certain pressure-temperature conditions. For example, sII methane hydrate at 250 MPa and sH methane hydrate at 600 MPa were reported [25]. Shu et al. (2011) reported a structural transition from sI methane to sII methane with space group  $Fd3m$  at 120 MPa and sH methane with space group  $P6_3/mmc$  at 600 MPa [26]. They reported decomposition of methane hydrate at high pressure above 3 GPa and formation of orientationally  $Fm3m$  structure methane and ice with space group  $Pn3m$  [26]. The formation of sII methane hydrate and coexistence of sI and s-II in the binary guest mixture of methane and ethane have also been reported [27–29]. In the real multicomponent natural gas systems, various hydrate structures or phases can form in the order of thermodynamic stability [30–33]. Heterogeneous and coexisting hydrate phases have been also rereported in the natural gas system [34].

### 3.1.2. Semi-clathrate hydrates

Water molecules and small gases such as methane and  $CO_2$  can form semi-clathrate hydrates. Unlike clathrate hydrates, semi-clathrate hydrates are crystalline compounds consisting of water and ionic or non-ionic compounds that can form with or without gas molecules. The

ionic substances are considered as both host and guest molecules that can physically attach to the water crystalline lattice through the hydrogen bond. The semi-clathrate hydrates are more stable than clathrate [35,36]. Since semi-clathrate hydrates are thermally stable at atmospheric pressure, they have many applications, including refrigeration fields [37,38], gas separation [39,40], and energy storage [41–45].

Various quaternary ammonium and phosphonium salts can form semi-clathrate hydrate. While tetra-*n*-butylammonium (TBA) and tetra-*n*-butylphosphonium (TBP) are the most common ionic elements used to form semi-clathrate hydrates [46–51], some other ionic elements have been reported such as tetra-iso-pentylammonium, tri-*n*-butyl sulfonium, and tetra-iso-amyl ammonium [52,53]. These ionic semi-clathrate hydrates are classified as a quaternary ammonium salt (QAS) and phosphonium salt hydrates. The equilibrium temperature of these semi-clathrate hydrates can be as high as 280 K–290 K at atmospheric pressure [54–58].

Four basic semi-clathrate hydrate structures were reported, including orthorhombic structure (space group  $Pbmm$ ), tetragonal structure (space group:  $P4_2/mmm$ ), tetragonal structure (space group  $P4_2/m$ ), and cubic structure ( $Pm3n$ ) [52]. These structures consist of different cages, such as pentagonal dodecahedral, tetrakaidecahedral, and pentakaidecahedral [59]. For example, TBA and TBP substances can enter the combined four cages, including two tetrakaidecahedra and two pentakaidecahedra [60,61].

Tetra-*n*-butylammonium bromide (TBAB) is one of the examples of TBA salt that has been used widely to form semi-clathrate in the form of  $C_{16}H_{36}N^+ \cdot Br^- \cdot 38H_2O$ . In this semi-clathrate hydrate, the anions substances (e.g.,  $Br^-$ ) can physically attach to the water crystalline lattice to construct the cavities. On the other hand, while the tetra-*n*-butylammonium substances (cations substances) can enter the cavities by breaking of cage structure, TBAB semi-clathrate hydrates can encage small gas molecules such as  $C_1$  [62],  $CO_2$  [63],  $H_2$  [64], and  $H_2S$  [65] through the empty dodecahedral cages [62].

While some researches show the promotion effect of TBAB in  $CO_2$  hydrate formation [66–72], TBAB may have an inhibitor effect at low concentration [73–77]. At a very high concentration of TBAB or in the presence of other quaternary ammonium salts, TBAB may not be involved in creating semi-clathrate hydrate (i.e., free ions of  $TBA^+$  and  $Br^-$ ) and act as an inhibitor [73,74]. Furthermore, the inhibition effect of diluted TBAB solution on  $CO_2$  gas hydrate formation was reported due to the impact of surface adsorption of  $TBA^+$  on water alignment at the gas water interface [78]. Temperature also affects the inhibition/promotion

effect of TBAB, i.e., while TBAB shows the inhibition effect in difluoromethane (HFC-32) + TBAB + water system above 289.4 K, it promotes the hydrate formation below 289.4 K [75].

The alkylamine hydrate is another class of semi-clathrate hydrates. The early studies of alkylamine hydrate were done by Pickering [79] together with some other studies related to alkylamine semi-clathrate hydrates [80–82]. The only exception to alkylamine semi-clathrate is tert-butylamine which occupies 17-hedra ( $4^35^96^27^3$ ) through canonical hydrate clathrate [83]. While the amine group in the alkylamine molecules can do hydrogen bonds to the water lattice, the alkyl chain functional groups stabilize the cavity [81]. Although the pure alkylamine forms semi-clathrate hydrates, the structural transition of semi-clathrate alkylamine hydrate to the canonical hydrates (e.g., sII hydrate) in the presence of secondary guest molecules (e.g., C<sub>1</sub>, H<sub>2</sub>) has been reported [84–87]. The alkylamine molecules are important because they could be potentially used for the CO<sub>2</sub> capture process using hydrate technology [88]. The CO<sub>2</sub> molecules are attracted to the alkylamine molecules due to the attraction forces between the carbon in CO<sub>2</sub> molecules and the negative charge in heteroatom nitrogen in the alkylamine molecules. This attraction force is relatively stronger than the attraction forces between CO<sub>2</sub> and oxygen in the water molecules [88]. Therefore, alkylamine molecules in the hydrate lattice can attract more CO<sub>2</sub> molecules.

### 3.2. CO<sub>2</sub> hydrate

#### 3.2.1. CO<sub>2</sub> clathrate hydrate structures

CO<sub>2</sub> can form both clathrate and semi-clathrate hydrates. Structure of CO<sub>2</sub> hydrate has been studied using X-ray diffraction [89–91], NMR spectroscopy [92], neutron powder diffraction [93,94], IR spectroscopy [95], and Raman spectroscopy [96,97]. These studies indicate sI CO<sub>2</sub> hydrate is the most stable hydrate structure. In sI hydrate, CO<sub>2</sub> molecule mainly occupies the large cages ( $5^{1,2}6^2$ ) while it can occupy small cages ( $5^{12}$ ), i.e., molecular size of CO<sub>2</sub> is close to the size of  $5^{12}$  cage, making it difficult to fit in small cages. Molecular dynamic simulation shows a rich orientation landscape of CO<sub>2</sub> molecules in sI [98]. Powder X-ray Diffraction show 99 % large cage occupancy and 69 % small cage occupancy in CO<sub>2</sub> sI hydrate [90]. CO<sub>2</sub> sI hydrate with the space group *Pm3n* can have different hydration numbers between 5.75 (if all cages are filled) and 7.67 (if only the large cages are filled) [89,99]. In fact, some cages may not be filled with CO<sub>2</sub> (particularly small cages,  $5^{12}$ ); therefore, a higher hydration number (>6) has been reported [89,92, 100–102].

Although CO<sub>2</sub> forms a stable sI, a transient formation of sII CO<sub>2</sub> hydrae with the growth of sI CO<sub>2</sub> hydrate was reported using neutron diffraction [103] and FTIR spectroscopy [104]. While sII transition occurs when some sI formers are mixed (e.g., CH<sub>4</sub>+C<sub>2</sub>H<sub>6</sub>), CO<sub>2</sub> doesn't form sII with another sI former [105]. However, sII hydrates form when CO<sub>2</sub> is mixed with other sII formers, such as propane [106]. The sII hydrate formation in the systems including CO<sub>2</sub>+N<sub>2</sub>+tetrahydrofuran (THF) [40], CO<sub>2</sub>+H<sub>2</sub>+THF [107], CO<sub>2</sub>+CH<sub>4</sub>+N<sub>2</sub> [108], CO<sub>2</sub>+CH<sub>4</sub>+THF [109,110], CO<sub>2</sub>+THF [96], and CO<sub>2</sub>+N<sub>2</sub> [111] was also reported.

CO<sub>2</sub> can also form sH hydrate as a co-guest. X-ray diffraction, Raman spectroscopy, and NMR indicate that CO<sub>2</sub> are trapped in the  $4^35^66^3$  cages and help the formation of sH hydrate in the CH<sub>4</sub>+CO<sub>2</sub>+Neohexane system [112,113]. The enclathration of CO<sub>2</sub> in sH hydrates has been also reported in N<sub>2</sub>+CO<sub>2</sub>+Neohexane [114], CH<sub>4</sub>+flue gas (CO<sub>2</sub>+N<sub>2</sub>) + Neohexane [113], CO<sub>2</sub>+N<sub>2</sub>+methylcyclopentane [115], CO<sub>2</sub>+methyl cyclopentane [116,117], CH<sub>4</sub>+CO<sub>2</sub>+N<sub>2</sub>+methylcyclopentane [118], N<sub>2</sub>+CO<sub>2</sub>+3,3-dimethyl-1-butanol [119], and CO<sub>2</sub>+3,3-dimethyl-2-butanone [120]. Although enclathration of CO<sub>2</sub> in sH hydrates was reported [92,114], a few studies showed that CO<sub>2</sub> is not a good help gas for some sH former (e.g., 3-methyl-1-butanol) [121,122].

In CO<sub>2</sub>-rich systems, the mole fraction of CO<sub>2</sub> significantly affects the stability of sH hydrate formation and may cause the structural transition [118,119,123]. The structural transition of sH to sI in the CO<sub>2</sub>-rich

systems has been reported in the CH<sub>4</sub>+CO<sub>2</sub>+Neohexane system [112, 123]. Uchida et al. pointed out that while the increase of CO<sub>2</sub> fraction reduces the stability of sH hydrates in the CH<sub>4</sub>+CO<sub>2</sub>+Neohexane system, it increases the thermodynamic stability of sI [112].

#### 3.2.2. CO<sub>2</sub> semi-clathrate hydrate structures

Tetra-*n*-butyl-ammonium salts (e.g., bromide (TBAB) [42,124,125], chloride (TBAC) [126,127], fluoride (TBAF) [128,129], nitrate (TBANO<sub>3</sub>) [130,131]) and tetra-*n*-butyl phosphonium salts (e.g., bromide (TBPB) [132,133], and chloride (TBPC) [40]) have been studied for engagement of CO<sub>2</sub> to semi-clathrate hydrates either in the pure CO<sub>2</sub> system or flue gas system (CO<sub>2</sub>+N<sub>2</sub>).

X-ray diffraction and Raman spectroscopic show the tetragonal hydrate structure formation with TBAC and orthorhombic hydrate structure formation with TBPB and TBPC [40]. TBAB, which is the most popular ionic substance, can form polymorphic phases consisting of orthorhombic and tetragonal hydrate structures in the CO<sub>2</sub> system [39]. In-situ Raman studies reveal that orthorhombic structures form at the onset of TBAB + CO<sub>2</sub> semi-clathrate hydrate formation, while tetragonal hydrate structures can form to make polymorphic phase [134]. In addition to the cation, the structure of semi-clathrate hydrate also depends on the type of anion [135], e.g., the CO<sub>2</sub> capture capacity in the TBAC + CO<sub>2</sub> hydrate structure is more than in the TBAB + CO<sub>2</sub> hydrate structure because CO<sub>2</sub> molecules can encapsulate in a planar distribution in the pentagonal dodecahedral cages [59]. CO<sub>2</sub> can occupy pentagonal dodecahedral cages as shown by X-ray diffraction in the TBAC + CO<sub>2</sub>+water system [59].

#### 3.2.3. CO<sub>2</sub> hydrate nucleation

Hydrate nucleation depends on many factors including composition, mixing rate, impurities/additives, driving force, and history effect [136–144]. Molecular dynamic simulations show that a high aqueous CO<sub>2</sub> concentration and adsorption of sufficient CO<sub>2</sub> molecules around hydration cages are the key factors in CO<sub>2</sub> hydrate nucleation [145]. Molecular dynamic simulations also show that higher guest concentration leads to a more structured hydration shell for the guest [146]. However, CO<sub>2</sub> hydrate formation from amorphous solid water and crystalline CO<sub>2</sub> is reported indicating CO<sub>2</sub> vapour pressure is not required for hydrate crystallization [147]. Formation of critical nucleation with a critical cluster size/radius is the first step of hydrate nucleation that is described by various mechanisms as summarized in Fig. 5. The classical nucleation theory calculates the hydrate nucleation point using Gibbs free energy analysis by assuming bulk-like properties of hydrate nucleus [148]. This theory assumes that hydrate nucleation can occur in the gas-liquid interface or supersaturated liquid water [149].

The microscopic view of hydrate nucleation and unknown hydrate structures in the classical approach leads to errors in free energy calculation and hydrate nucleation point. Therefore, other theories are developed by considering of intermolecular interactions between water and gas molecules. Labile cluster nucleation hypothesis suggests that the interaction between water molecules and dissolved gas in aqueous phase makes the labile clusters surrounding the gas molecules [150]. This theory says hydrate nucleation will occur when both type of cavities for sI or sII are formed. The interface nucleation theory was also proposed based on labile clusters formation only on the vapour side of gas-water interface [151]. In this theory, when gas molecules are adsorbed to the interface and moved to the right position, the partially open cages are formed and then completed.

Molecular dynamic simulation of CO<sub>2</sub> hydrate nucleation shows another mechanism called local structuring nucleation [152]. In this theory, CO<sub>2</sub> molecules are arranged locally by the thermal fluctuation rather than arrangement of water molecules. This local arrangement of gas molecules induces the ordering of water molecules that leads to hydrate nucleus formation.

The study of amorphous precursors in CO<sub>2</sub> hydrate nucleation using

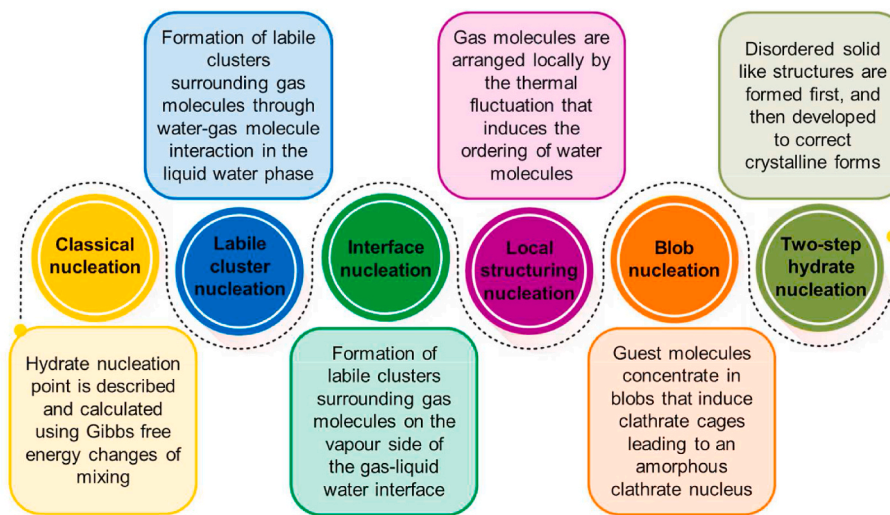


**Fig. 5.** Various gas hydrate nucleation mechanisms.

molecular dynamic simulation proposed the blob nucleation mechanism [153]. In blob nucleation mechanism, guest molecules concentrate in blobs which are in equilibrium with solution. These blobs induce the cages that lead to an amorphous clathrate nucleus. This theory uses both features of local structuring and labile cluster mechanisms [153].

In the two-step mechanism hydrate nucleation, the disordered solid-like structures start to form as an amorphous phase [154]. This intermediate state is then processed to evolve correct hydrate structure. Moreover, some researchers proposed multiple pathways for hydrate nucleation including direct nucleation [155–157]. In addition to different hydrate nucleation mechanisms, various models have been introduced to describe CO<sub>2</sub> hydrate nucleation based on different theories, including crystallization [158], classical nucleation [159], and phase field theory [160,161]. One model was proposed by Natarajan et al. to predict the induction time by crystallization considerations [158]. In this model, the induction time is an exponential dependence of driving force (fugacity difference). Another model was proposed by Kvamme established based on phase field theory to describe CO<sub>2</sub> hydrate nucleation rate [160].

#### 3.2.4. CO<sub>2</sub> hydrate growth

Growth kinetics of CO<sub>2</sub> hydrate can be studied experimentally by observing the changes in the concentration of dissolved CO<sub>2</sub> in water and the rate of hydrate formation. The rate of CO<sub>2</sub> hydrate growth is influenced by several factors, including the concentration of dissolved CO<sub>2</sub>, CO<sub>2</sub> concentration of the gas mixture, diffusion of water and guest molecules, temperature, pressure, mixing, heat transfer, and the presence of chemicals/additives. At low concentrations of dissolved CO<sub>2</sub>, growth rate of CO<sub>2</sub> gas hydrate is slow, but it increases with increasing CO<sub>2</sub> concentration. Lower temperatures and higher pressures also increase the growth rate of CO<sub>2</sub> hydrate. It has been demonstrated that while decreasing of temperature can significantly increase the CO<sub>2</sub> hydrate growth rate, the pressure has little effect on growth rate [162].

The growth of CO<sub>2</sub> gas hydrate is a complex process that involves several stages. First, small crystals of CO<sub>2</sub> hydrate are formed through a process called nucleation as described before. Next, these crystals grow as additional water molecules and CO<sub>2</sub> are added to the crystal lattice. Finally, the crystals may merge to form larger crystals through the agglomeration process. Various mathematical models have been developed to describe the kinetics of gas hydrate growth, which are based on different controlling mechanisms, including heat transfer, mass transfer, and intrinsic kinetics.

In the hydrate growth models with heat transfer rate dominated, temperature has a highest impact on CO<sub>2</sub> hydrate growth rate which is

controlled by conductive and convection heat transfer [163,164]. Uchida et al. proposed a model (Equation (1)) for CO<sub>2</sub> hydrate film growth which is controlled by temperature gradient [165].

$$\vartheta\lambda^{-1} = (L\rho_c r_c)^{-1} \Delta T \quad \text{Equation 1}$$

where  $\vartheta$  is rate of CO<sub>2</sub> hydrate film,  $\lambda$  is the thermal conductivity,  $L$  is latent heat of the hydrate formation,  $\rho_c$  is CO<sub>2</sub> hydrate density, and  $\Delta T$  is the temperature difference. Peng et al. also demonstrated that CO<sub>2</sub> hydrate growth rate depends on temperature and NaCl concentration [166].

In the mass transfer dominated hydrate growth rate, CO<sub>2</sub> gas dissolution is the rate-dominated step. Zhou and Ferreira proposed Equation (2) for mass growth rate of CO<sub>2</sub> hydrate ( $G$ ) which is controlled by mass transfer [167] ( $k_l$  is CO<sub>2</sub> mass transfer coefficient from bulk liquid to the crystal,  $\rho_{sol}$  is solution density,  $A_h$  is hydrate layer area,  $x_b^{CO_2}$  and  $X_{int}^{CO_2}$  are the CO<sub>2</sub> mole fraction in the bulk liquid and liquid-crystal layer in equilibrium respectively).

$$G = k_l \rho_{sol} A_h (x_b^{CO_2} - X_{int}^{CO_2}) \quad \text{Equation 2}$$

Intrinsic kinetics of CO<sub>2</sub> hydrate can be also investigated by eliminating the effect of mass and heat transfer using stirred tank reactor [168–170]. In intrinsic model, the fugacity difference between CO<sub>2</sub> dissolved gas and three-phase equilibrium ( $f - f_{eq}$ ) is proposed as an overall driving force for hydrate crystallization [170]. The chemical potential difference or mole difference was also introduced as a driving force [171,172]. Clark and Bishnoi used Equation (3) to describe the intrinsic kinetics of CO<sub>2</sub> hydrate [168] ( $R_y(t)$  is reaction rate,  $K^*$  is overall rate constant around hydrate particle, and  $\mu_2$  is second moment of particle size distribution).

$$R_y(t) = \pi K^* \mu_2 (f - f_{eq}) \quad \text{Equation 3}$$

When mass and heat transfer resistance are negligible, the overall rate constant ( $K^*$ ) is approximately equal to intrinsic rate constant of hydrate formation. Clark and Bishnoi reported the intrinsic rate constant of CO<sub>2</sub> hydrate in the range of  $3.214 \times 10^{-3}$ –  $6.423 \times 10^{-3}$  (mole / m<sup>2</sup>Pa s) [168].

Heat transfer, mass transfer, and intrinsic kinetics cannot be ignored and may control the CO<sub>2</sub> hydrate growth simultaneously [173]. Ota et al. described the kinetics of CO<sub>2</sub> gas hydrate by considering both controls mechanisms of mass transfer and intrinsic kinetics [174]. One such model is introduced by Sarshar et al. which describes the growth of CO<sub>2</sub> hydrate crystals in terms of heat transfer, mass transfer, and intrinsic kinetics [175].

### 3.2.5. CO<sub>2</sub> hydrate properties

Thermophysical properties and bulk properties of CO<sub>2</sub> hydrate are essential for studying gas hydrate in the sediment and simulating carbon sequestration using gas hydrate. CO<sub>2</sub> hydrate density is required for accurate modelling and simulation of carbon injection into cold saline aquifers or deep ocean storage of CO<sub>2</sub>, where the density of CO<sub>2</sub> hydrate plays an essential role in determining the final distribution of CO<sub>2</sub>. To measure the density of CO<sub>2</sub> hydrate and understand its relationship with temperature and pressure, several steps are involved. Initially, the structure and composition of CO<sub>2</sub> hydrate are determined through experimental techniques like X-ray diffraction or theoretical techniques such as Monte Carlo Simulation. This provides crucial information about the lattice parameter and composition which are required for density estimation. Subsequently, the density of CO<sub>2</sub> hydrate can be estimated by considering factors such as cage occupancy and the temperature-pressure dependence of unit-cell parameters. By analysing how these parameters vary with temperature, the density-temperature/pressure relationship of CO<sub>2</sub> hydrate can be determined. Density of CO<sub>2</sub> hydrate measured by different techniques at some conditions are listed in Table 1.

As mentioned, to estimate CO<sub>2</sub> hydrate density, it is essential to know the lattice parameter and composition. As pressure increases, CO<sub>2</sub> molecules tend to fill both small and large cages in sI. While hydrostatic pressure causes lattice compression and decreasing hydration number, the lattice parameter increases with temperature due to thermal expansion. The lattice parameter of CO<sub>2</sub> hydrate as a function of pressure and temperature is shown in Fig. 6. As shown in Fig. 6 (a), lattice parameter of CO<sub>2</sub> hydrate can increase from 11.83 Å at 8 K to 11.97 Å at 270 K at atmospheric pressure.

Some other thermos-physical properties of CO<sub>2</sub> hydrate reported in the literature are listed in Table 1. While molecular dynamic simulation was used to estimate the dissociation heat of CO<sub>2</sub> hydrate [127], experimental techniques using a calorimeter and Clausius Clapeyron equation have been used to measure the dissociation heat as listed in Table 1. Dissociation heat of CO<sub>2</sub> hydrate could be in the range of 50–70 kJ mol<sup>-1</sup>, and is directly related to pressure, temperature, and hydration number. The hydration number of CO<sub>2</sub> hydrate as a function of temperature at different pressure is also plotted in Fig. 7 (b). The results reveal that the hydration number decreases at low temperature and high pressure, indicating that CO<sub>2</sub> molecules tend to fill both small and large cages in sI.

Furthermore, heat capacity of hydrate is a vital parameter to control the CO<sub>2</sub> hydrate dissociation when the thermal dissociation of hydrate occurs in the sediment. While there are several data for the heat capacity of hydrates (e.g., methane) [190], there are limited data for CO<sub>2</sub> hydrate. The specific heat capacity of CO<sub>2</sub> hydrate predicted by PVTsim is shown in Fig. 7 (a), which is in the range of values predicted by Mathews et al. [191]. Ning et al. also used molecular dynamics to predict the specific heat capacity of CO<sub>2</sub> hydrate between ~2100–2700 (J Kg<sup>-1</sup> K<sup>-1</sup>) [188] which is much higher than Mathews et al. [191]. Therefore,

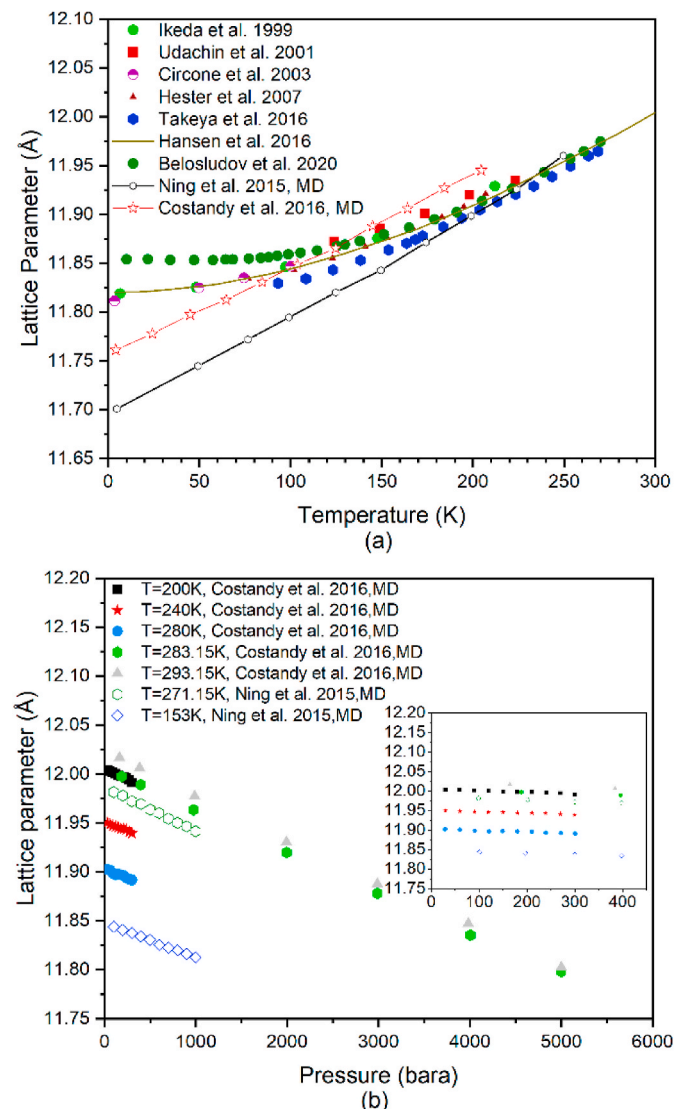


**Fig. 6.** Lattice parameter of CO<sub>2</sub> hydrate (a) as a function of temperature at atmospheric pressure [89,91,183–189] (b) as a function of pressure at constant temperature [188,189]. (MD: molecular dynamic).

further research is required to experimentally measure CO<sub>2</sub> hydrate heat capacity.

Interfacial properties in CO<sub>2</sub>-water-hydrate system, including contact angle and interfacial tension (IFT), play an essential role in hydrate nucleation, crystallization, and growth. The experimental observation

**Table 1**  
Reported thermo-physical properties of CO<sub>2</sub> hydrate.

Hydration Number	Density (Kg/m <sup>3</sup> )	Dissociation Heat (kJ/mole)	Temperature (K)	Pressure (bara)	Method	Reference
6.2	1140		173		X-ray diffraction	Udachin et al. [89]
6.5	1105		268		X-ray diffraction	Takeya et al. [91]
5.75	1126.2–1179.9		150–280	40–500	Monte Carlo Simulation	Ferdows and Ota [127],
7.67	1050.1–1093.3					
7.3	1090–1110	35.57	285.15	300	Heat Exchange	Aya et al. [176]
7.3	1110	58.2–61.5	273–283	1	Clausius Clapeyron	Bozzo et al. [177]
5.9–6		66.6–69.6	277.15–281.15	19.9–33.4	Clausius Clapeyron	Fournaison et al. [178]
5.75–6.4		58.2–62.5	274.15–282.15	13.7–38.6	Clausius Clapeyron	Anderson [99]
		56.85–75.37	273.15–282.06	10.5–36	Clausius Clapeyron	Sabil et al. [179]
6.21		57.66	273.15		Clapeyron	Yoon et al. [102]
6.6–7.9		63.1–70.8	275.3–279.9	15.9–28.6	Clapeyron	Lirio et al. [180]
		50.3–58.4	276–280	17–31	Clapeyron	Ohgaki et al. [181]
7.23		65.22 ± 1.03	273.65	1	Calorimetry	Kang et al. [182]

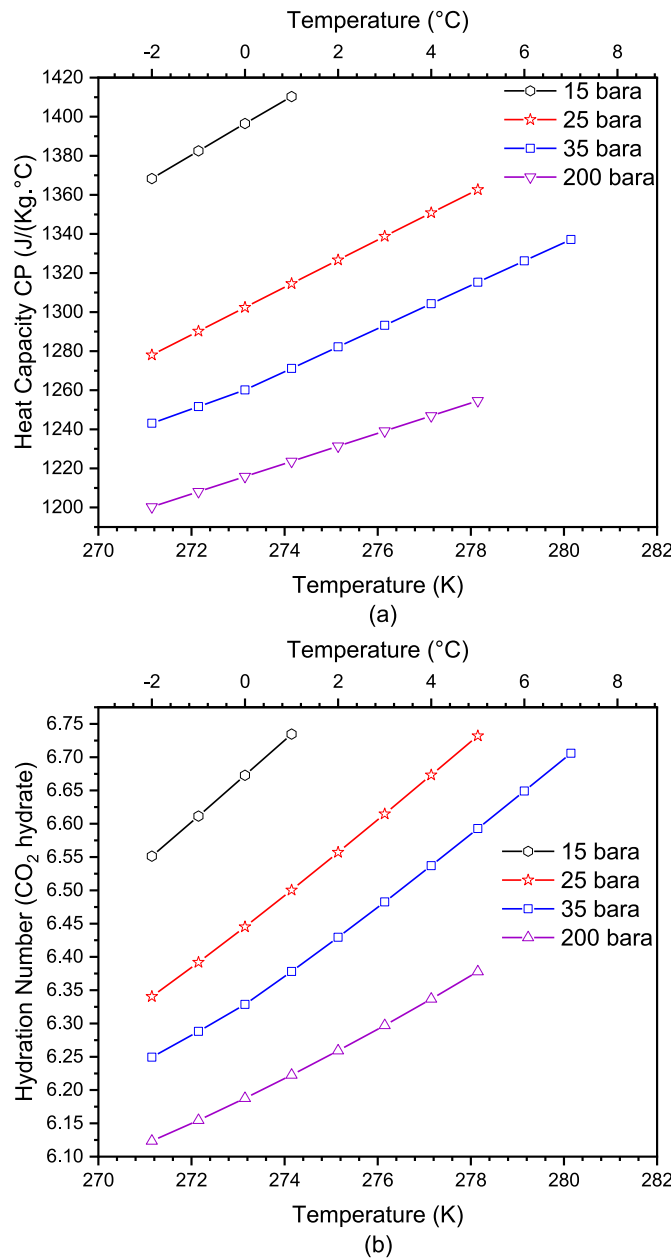


**Fig. 7.** Specific heat capacity ( $C_p$ ) and hydration number for  $\text{CO}_2$  sI hydrate predicated by PVTsim using the SRK-CPA equation of state.

using the pendant drop method indicates that the summation of interfacial tension between liquid  $\text{CO}_2$  and  $\text{CO}_2$  hydrate and between water and  $\text{CO}_2$  hydrate is less than between water and liquid  $\text{CO}_2$  [192]. Further studies about the effect of IFT on the kinetics of  $\text{CO}_2$  hydrate reveal that hydrate growth rate increases as IFT decreases [193]. Interfacial phenomena have also a crucial role in hydrate inhibition where thermodynamic hydrate inhibitors (e.g., methanol) can change the solubility of  $\text{CO}_2$  and hydrocarbon components [194,195].

### 3.2.6. Phase equilibria: $\text{CO}_2$ hydrate

Various experimental and numerical methods have been used to explore the equilibrium condition of  $\text{CO}_2$  hydrate. The hydrate dissociation point can be determined using various techniques [196] including visual observation or graphical analysis through isochoric [197], isothermal [198], or Isobaric [199] process using autoclave cell [30], differential scanning calorimetry [200], and microfluidic device [201]. Among the different techniques to measure hydrate dissociation point,

nonvisual techniques combined with step heating in the isochoric approach is the most popular technique [202]. In this method, the hydrate dissociation point is measured by the intersection of cooling and heating curves which can be determined by measuring a few equilibrium points. However, Aminnaji et al. (2021) indicated that various clear heating curve slopes could be observed in the multicomponent systems due to the presence of various hydrate structures, therefore, the step heating method could result in the wrong equilibrium dissociation point [30,196].

Furthermore, numerical modelling using equation of state (EoS) has been used to predict gas hydrate equilibrium state [203]. A multiphase flash using CPA combined with Peng–Robinson was used to describe the fluid phases and vapour-liquid-hydrate equilibrium [204]. It is concluded that CPA can better predict the phase equilibria of  $\text{CO}_2$  hydrate [205]. In fact, the CPA considers the chemical/quasi-chemical associative hydrogen bonds contribution through the associating sites and strength. Particularly, for  $\text{CO}_2$  hydrate modelling, the guest–guest interactions should not be ignored in CPA due to the rich orientation landscape of  $\text{CO}_2$  molecules in structure I hydrate [98].

To predict hydrate equilibrium using EoS, it is required to calculate the chemical potential and fugacity of molecules in the hydrate phase. This is achieved by various models that calculate the molecule-cell interaction potential while assuming spherically symmetric conditions, i.e., Zhang et al. compared the accuracy of vdW-P model, Parrish–Prausnitz model, John–Holder mode, and Chen–Guo model for the prediction of  $\text{CO}_2$  gas hydrate equilibrium curve [206]. However, density functional theory (DFT) calculations for  $\text{CO}_2$  gas hydrates shows that  $\text{CO}_2$  molecule - cell interaction potential is anisotropic and asymmetric. Therefore, spherical approximations for guest molecule–hydrate interaction may not be sufficient for  $\text{CO}_2$  hydrates [207].

Molecular dynamics (MD) simulation has been also used to measure the phase equilibrium [208]. MD was used to study  $\text{CO}_2$  hydrate growth/dissociation and the mechanism involved in the guest involvement or replacement in the hydrate crystals [209–212]. Three phase equilibrium of hydrate + liquid water + liquid  $\text{CO}_2$  was analysed from 2 MPa to 500 MPa using the MD simulation [213]. It is pointed out that a positive deviation from Lorentz–Berthelot combining rules must be considered for accurate prediction [213]. Different water and  $\text{CO}_2$  molecular models (TIP4P/Ice, TIP4P/2005, SPC/E, SPC/Fw) were also examined to predict  $\text{CO}_2$  hydrate stability and dissociation [214]. The growth and equilibrium temperature of  $\text{CO}_2$  hydrate up to 100 MPa were also analysed using MD simulation [215]. It is demonstrated that although sI hydrate is stable at below 100 MPa, the emergence of unstable medium-sized  $4^{1}5^{10}6^2$  cages may affect the  $\text{CO}_2$  hydrate growth [215].

Figs. 8 and 9 show experimental data illustrating the phase equilibrium and hydrate phase boundary for  $\text{CO}_2$ +water system at low and high pressure, respectively. The  $\text{CO}_2$  liquid-gas equilibrium line and ice melting equilibrium line divide the global phase diagram of  $\text{CO}_2$  into different sections that are equilibrated with  $\text{CO}_2$  hydrate. The trend of  $\text{CO}_2$  hydrate equilibrium curve depends on the presence of other phases, i.e., as shown in Fig. 8, the quadruple points of  $Q_1$  and  $Q_2$  change this trend significantly.

As shown in Fig. 9, the re-entrant phenomenon of  $\text{CO}_2$  hydrate is observed at a very high pressure. An equilibrium temperature of 294 K at 328 MPa is reported as a maximum temperature that  $\text{CO}_2$  hydrates can form [222]. At very high pressure, the hydrate structure shrinks due to the reduction in the size of hydrate cages, so they become too small to stabilize the gas molecules. Hydrate re-entrant behaviour of  $\text{CO}_2$  is also indicated at high pressure by MD simulation [213]. The s-I  $\text{CO}_2$  clathrate hydrate can be stable up to 0.7–0.8 MPa as shown in Fig. 9. However, above this pressure, s-I  $\text{CO}_2$  hydrate is no longer stable and a new high-pressure phase (filled ice-like framework) forms between 0.8 and 1 GPa [223].

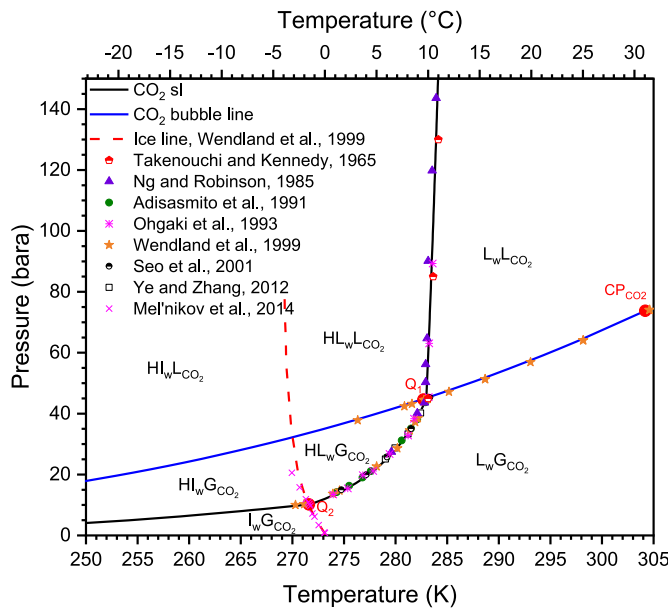


**Fig. 8.** Hydrate phase boundary and phase equilibrium for  $\text{CO}_2$ -water up to 150 bara. Black and blue solid lines are  $\text{CO}_2$  hydrate phase boundary and  $\text{CO}_2$  liquid-vapour equilibrium predicted by PVTsim. Dashed red line is ice melting equilibrium line for water saturated with  $\text{CO}_2$  [216]. The other equilibrium data points are taken from Refs. [181,197,216–221]. H=CO<sub>2</sub> hydrate, L<sub>CO<sub>2</sub></sub>=Liquid CO<sub>2</sub>, G<sub>CO<sub>2</sub></sub>=Gas CO<sub>2</sub>, L<sub>w</sub>=liquid water, I<sub>w</sub>=Ice water, CP=critical point, Q=quadruple point. (For interpretation of the references to colour in this figure legend, the reader is referred to the Web version of this article.)

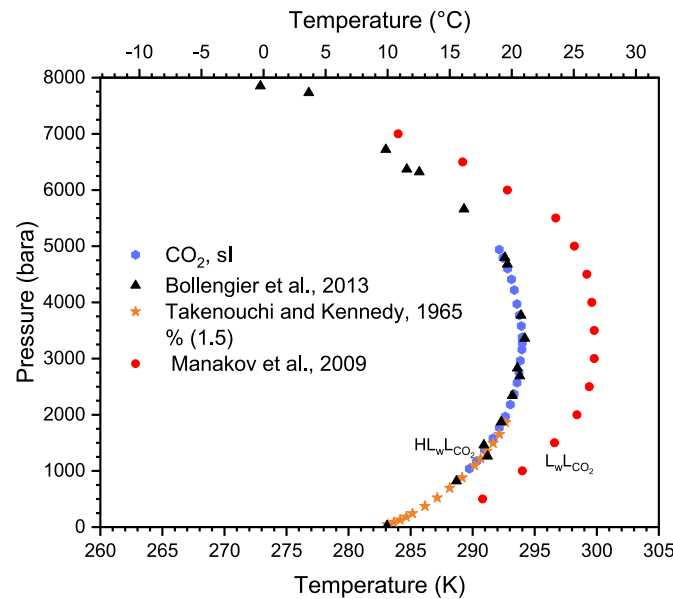


**Fig. 9.** Hydrate phase boundary for the system  $\text{CO}_2$ -water up to 8000 bara. The equilibrium data points are taken from Refs. [222,223,218,224].

### 3.2.7. Phase equilibria: $\text{CO}_2$ replacement in methane hydrate

Phase equilibria and hydrate phase boundary of CO<sub>2</sub> with other gas components (e.g., methane and nitrogen) are discussed in this section. Fig. 10 shows the hydrate phase boundary and phase envelope of CO<sub>2</sub>+CH<sub>4</sub> gas mixture at different compositions. Hydrate phase boundary shifts to the lower pressure at a particular temperature by adding more stable guest molecules (e.g., adding more CO<sub>2</sub> to CH<sub>4</sub>). At lower pressure, hydrate pressure formation of CO<sub>2</sub> is lower than CH<sub>4</sub> at a particular temperature. It indicates that CO<sub>2</sub> molecules are more

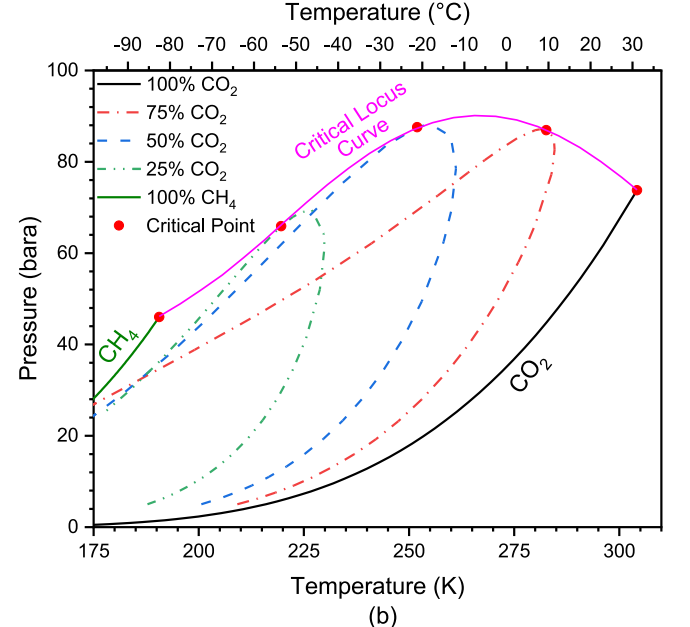
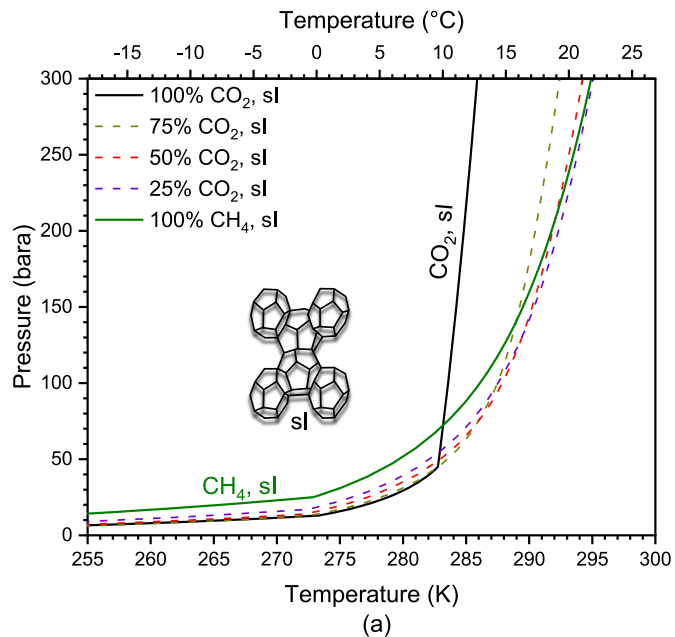


**Fig. 10.** (a) Hydrate phase boundary and (b) Phase envelop for mixture of CO<sub>2</sub> and CH<sub>4</sub> predicted by PVTsim.

thermodynamically stable than CH<sub>4</sub> molecules in hydrate sl. In contrast, at higher pressure where CO<sub>2</sub> is liquid, the hydrate pressure formation of CO<sub>2</sub> becomes more than CH<sub>4</sub> at a particular temperature. This has come up with the idea of CO<sub>2</sub> injection into the hydrate reservoir to be replaced with methane in the clathrate cages. This process of methane replacement with CO<sub>2</sub>, which is an exothermic process [225], not only helps with carbon storage but also induces methane production from gas hydrate reservoir. Injection of flue gas (CO<sub>2</sub>-N<sub>2</sub> mixture) into the hydrate reservoir shows some promising advantages over pure CO<sub>2</sub> injection [226]. So, various studies have investigated the thermodynamic process [227] and hydrate stability zone of flue gas with methane [228–232]. A comparison of hydrate phase boundaries for CH<sub>4</sub>, CO<sub>2</sub>, N<sub>2</sub>, and a mixture of flue gas is shown in Fig. 11.

### 3.2.8. CO<sub>2</sub> hydrate in the presence of other components

The syngas, flue gas, and biogas usually consist of other components

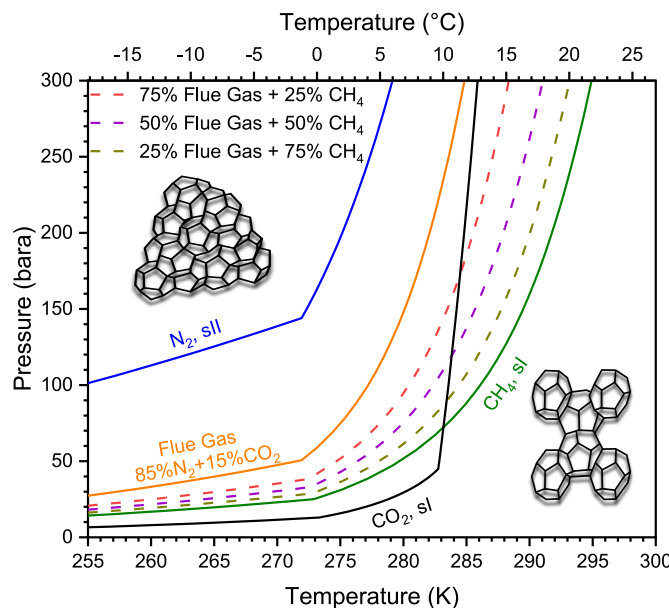


**Fig. 11.** Hydrate phase boundary for CH<sub>4</sub>, CO<sub>2</sub>, N<sub>2</sub>, and flue gas predicted by PVTsim.

such as NOx (nitrogen oxides), SO<sub>2</sub> (sulfur dioxide), O<sub>2</sub> (oxygen), CO (carbon monoxide), H<sub>2</sub>S (hydrogen sulfide), H<sub>2</sub>O, Hg (Mercury), As (Arsenic), Ar (Argon), H<sub>2</sub> (hydrogen), etc. Those impurities that can form a more thermodynamically stable hydrate than CO<sub>2</sub> shift the hydrate phase boundary of CO<sub>2</sub> hydrate to the lower pressure. For example, the molecular dynamic simulation shows that the clathrate hydrate of H<sub>2</sub>S and SO<sub>2</sub> is more stable than CO<sub>2</sub> hydrate, therefore, a high content of these impurities can reduce the efficiency of carbon capture and storage by hydrate technology [233]. The molecular dynamic simulation also shows that while SO<sub>2</sub> tends to encage the large cages, H<sub>2</sub>S tends to encage the small cages [233] which has been confirmed by others [234–236]. The Laser Raman Spectroscopy shows SO<sub>2</sub> molecules can be encaged in both small and large cages in CO<sub>2</sub> hydrate lattice and increase the stability of CO<sub>2</sub> hydrates [237]. In contrast, those impurities that are less stable than CO<sub>2</sub> hydrate shift the hydrate phase boundary to the higher pressure. For example, N<sub>2</sub>, O<sub>2</sub>, and Ar hydrates are less thermodynamically stable than CO<sub>2</sub> hydrates.

Fig. 12 shows the phase boundary of some pure components that potentially exist in the flue gas. The hydrate phase equilibria of CO<sub>2</sub> rich system in the presence of some impurities (e.g., N<sub>2</sub>, CH<sub>4</sub>, O<sub>2</sub>, Ar, and CO) were measured experimentally and modelled using CPA by Chapoy et al. [238]. The hydrate phase boundary of binary systems of CO<sub>2</sub>-N<sub>2</sub> and CO<sub>2</sub>-CH<sub>4</sub> (or a mixture of CO<sub>2</sub>+N<sub>2</sub>+CH<sub>4</sub>) in the water or brine were also experimentally measured and predicted by Herri et al. [239], Zheng et al. [240,241], Legoix et al. [242], Zang et al. [243], Li et al. [244], and Chazallon and Pirim [245].

Impurities in the flue gas can form different hydrate structures. Both nitrogen [246] and Argon [247] are known to form hydrate structure II. The neutron powder diffraction also confirms the formation of oxygen structure II hydrate [248]. In contrast, hydrogen sulphide and methane tend to occupy the tetrakaidecahedrons ( $5^{1,2}6^2$ ) and dodecahedrons ( $5^{1,2}$ ) cages, respectively, and they form structure I hydrate [249,250]. In-situ Raman spectroscopy shows that the selectivity of CO<sub>2</sub> capture in structure II is lower than in structure I in CO<sub>2</sub>+N<sub>2</sub> system [245].

Phase equilibrium of CO<sub>2</sub> hydrate has also been investigated in the presence of other components, such as cyclopentane and hydrogen. The hydrate phase equilibrium of CO<sub>2</sub> and cyclopentane is experimentally measured and modelled by Babakhani et al. [251]. They reported that various hydrate structures (structures I and II) can form in CO<sub>2</sub>+cyclopentane mixture [251]. The CO<sub>2</sub>+H<sub>2</sub> hydrate has also been

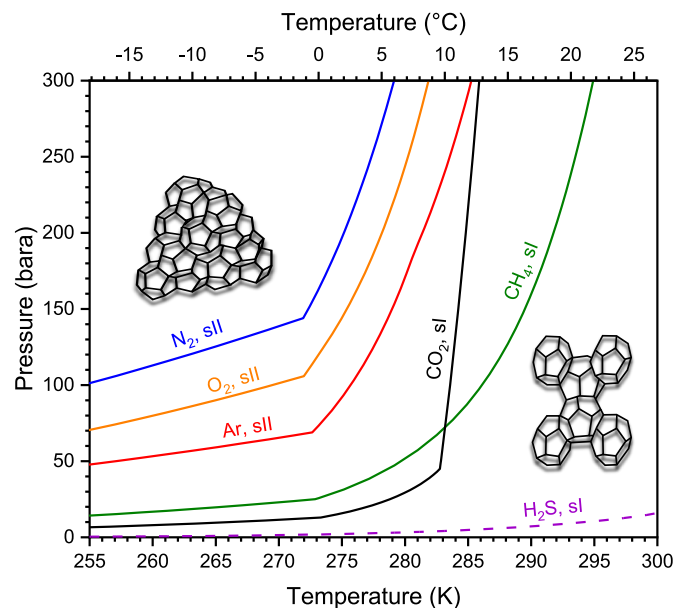


**Fig. 12.** Hydrate phase boundary for pure methane (CH<sub>4</sub>), carbon dioxide (CO<sub>2</sub>), nitrogen (N<sub>2</sub>), Oxygen (O<sub>2</sub>), argon (Ar), and hydrogen sulphide (H<sub>2</sub>S) predicted by PVTsim.

studied due to its different applications, including increasing gas recovery by injection of CO<sub>2</sub>+H<sub>2</sub> mixture into the hydrate reservoir [252–254], hydrogen hydrate storage [255], and CO<sub>2</sub> separation [256]. Xie et al. showed that the small concentration of H<sub>2</sub> and N<sub>2</sub> enhances the effectiveness of CO<sub>2</sub> replacement in methane hydrate reservoir [257]. The Raman, neutron, and x-ray show that pure hydrogen form structure II hydrate [258]. However, Xie et al. demonstrated that H<sub>2</sub> can be encaged both in  $5^{1,2}$  and  $5^{1,2}6^2$  cages in the form of CO<sub>2</sub>+H<sub>2</sub> structure I [259, 260]. They reported the coexisting of CO<sub>2</sub> and H<sub>2</sub> in the large cavity of structure I ( $5^{1,2}6^2$ ) [259]. It is also reported that several hydrogen molecules can occupy the cages in the hydrate structures [261]. Skiba et al. experimentally measured the hydrate phase equilibria of the CO<sub>2</sub>+H<sub>2</sub> mixture and the hydrogen solubility at different H<sub>2</sub> concentration [262].

It has been shown that the impurities of N<sub>2</sub> and CH<sub>4</sub> can reduce CO<sub>2</sub> storage capacity due to the change in the hydrate stability zone [263]. The impurities and hydrates can also change the fluid properties. The solubility measurement under the hydrate-liquid-vapour equilibrium has been investigated by many researchers for various CO<sub>2</sub>+impurities systems, including CO<sub>2</sub>+CH<sub>4</sub> [264,265], CO<sub>2</sub>+N<sub>2</sub> [266], and CO<sub>2</sub>+CH<sub>4</sub>+C<sub>2</sub>H<sub>6</sub> [267]. An experimental investigation and thermodynamic models were implemented by Chapoy et al. to investigate the effect of impurities such as N<sub>2</sub>, O<sub>2</sub>, and Ar on the phase behaviour of CO<sub>2</sub> hydrate [268]. They reported that these impurities can change some thermophysical properties of pure CO<sub>2</sub> by decreasing the density (up to 35 %) and water dissolution (10–30 % lower than pure CO<sub>2</sub>) [268]. There are some other impurities (e.g., metal nanoclusters [269], nanoparticles [270], TBAB [271], THF [272], etc.) that could be deliberately used to change the hydrate stability region or promote CO<sub>2</sub> hydrate formation, which are discussed in next section.

#### 4. Hydrate-based carbon capture

CO<sub>2</sub> capture could be undertaken in pre-combustion, oxy-fuel combustion, or post-combustion. In pre-combustion, CO<sub>2</sub> is removed from fuels before utilisation. For example, the process involves the partial oxidation of coal using air or oxygen to produce a synthesis gas composed of hydrogen, carbon monoxide, and a small amount of methane. In a gas clean-up stage, CO is converted to CO<sub>2</sub>, resulting in a

synthesis gas with CO<sub>2</sub> and H<sub>2</sub> concentrations of around 40 % and 50 %, respectively. The CO<sub>2</sub> is then removed from the gas resulting in H<sub>2</sub>-rich gas [273,274].

In oxy-fuel combustion (combustion in an oxygen-enriched atmosphere) exhaust gas with high concentrations of CO<sub>2</sub> and water vapour with minimum nitrogen are produced. This high content of CO<sub>2</sub> gas can be removed through the CO<sub>2</sub> drying and compression. However, to produce oxygen for combustion, the air separation process is required, i.e., oxygen purity of approximately 95 % [275].

On other hand, post-combustion technologies are often preferred for existing conventional power units [276]. In this process, carbon capture process is employed after fuel combustion to remove CO<sub>2</sub> from the low concentration of CO<sub>2</sub>. For example, a typical exhaust gas from coal-based power plants consists of N<sub>2</sub>, CO<sub>2</sub>, O<sub>2</sub>, H<sub>2</sub>O, and some impurities (e.g., SO<sub>2</sub>, and NO<sub>2</sub>). The CO<sub>2</sub> partial pressure and concentration (e.g., 13–15 %) are low in the flue gas, therefore, it results in a low driving force for carbon capture [275,277,278]. The processes of CO<sub>2</sub> separation in oxy-fuel combustion, post-combustion, and pre-combustion are shown in Fig. 13. The aforementioned approaches for carbon capture have different physical and chemical processes as shown in Fig. 14.

Among the various techniques, hydrate-based carbon capture (HBCC) is one of the carbon capture technologies, which is discussed in this section.

#### 4.1. Hydrate-based decarbonisation fundamentals

Hydrate-based CO<sub>2</sub> separation is a promising technology that uses gas hydrates to separate CO<sub>2</sub> from gas mixtures [19,279]. Hydrate-based technology can also be applied to separate other gases such as Xenon from Noble Gas Mixtures [280]. The process involves the formation of CO<sub>2</sub> hydrates, followed by dissociation, effectively separating CO<sub>2</sub> from a gas mixture (Fig. 15). Due to the differences in the phase equilibria of

CO<sub>2</sub> in the presence of the other gases, CO<sub>2</sub> is trapped in the hydrates and CO<sub>2</sub> separation can occur effectively [281]. This process typically occurs at low temperature and high-pressure [282]. The amount of CO<sub>2</sub> that can be accommodated in the CO<sub>2</sub> hydrates depends on several factors, such as pressure, temperature, and the composition. For example, Raman spectroscopy was used to investigate the trapping efficiency of HBCC technology for CO<sub>2</sub>-N<sub>2</sub> and CO<sub>2</sub>-CO [283]. The findings indicated a higher efficiency for CO<sub>2</sub>-N<sub>2</sub> mixture at low CO<sub>2</sub> concentration.

This method offers several opportunities, including a cost-effective (low capital investment) and energy-efficient alternative to traditional methods [284,285]. Moreover, applying the hydrates as a transport medium for CO<sub>2</sub> is another economic benefit [286,287]. Low energy requirements of HBCC and the possibility of using waste heat sources to feed and drive the process attract lots of attention in research society [288,289]. In a method developed by Obara & Tanaka (2021), the waste heat from nuclear power plants has been used to operate a hydrate heat cycle [288].

Further application of the HBCC is in natural gas processing, in which this technology can be used to remove CO<sub>2</sub> from natural gas streams to enhance purity [290,291]. This application is also extended to separating CO<sub>2</sub> from fuel or flue gases emitted from power plants, cement factories, and other industrial sources [226,279,292,293].

One of the challenges in HBCC is how to increase the rate of hydrate formation. The importance of intricate interaction between CO<sub>2</sub> and water molecules in the hydrate structure can dictate the efficiency of CO<sub>2</sub> capture process. Different scale study of HBCC is critical in enhancing our understanding of this process. By exploring at micro to meso-scale, the research community can gain insights into fundamental governing mechanisms, including hydrate formation, growth, and dissociation. In terms of CO<sub>2</sub> hydrate promoters, experimental data on micron-scale crystallographic features are lacking, creating a gap between single scales such as macroscopic temperature-pressure variations

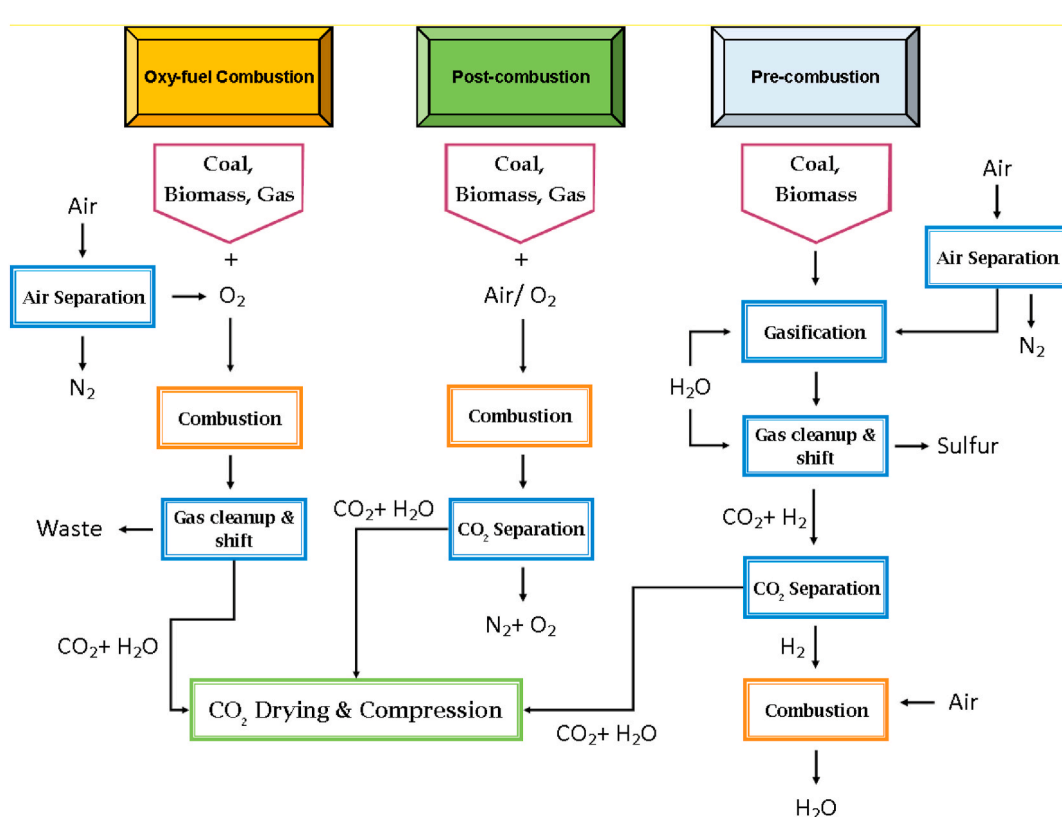


**Fig. 13.** CO<sub>2</sub> separation in oxy-fuel combustion, post-combustion, and pre-combustion.

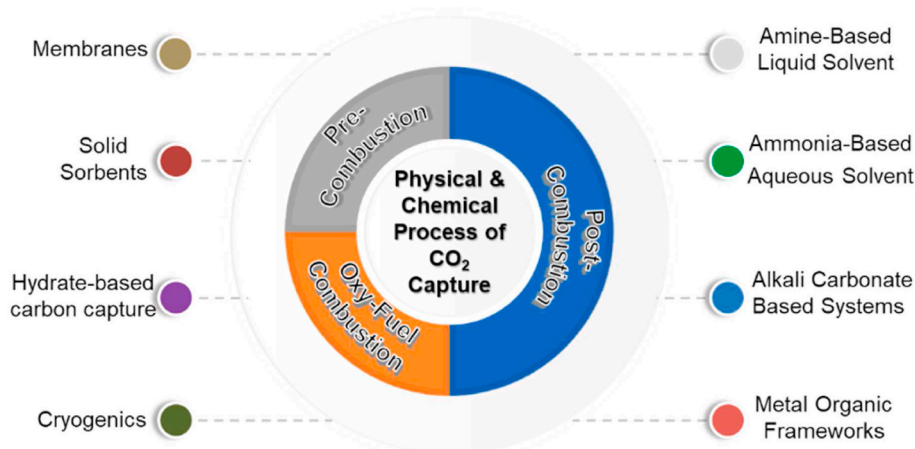


**Fig. 14.** Various physical and chemical processes involved in CO<sub>2</sub> capture.

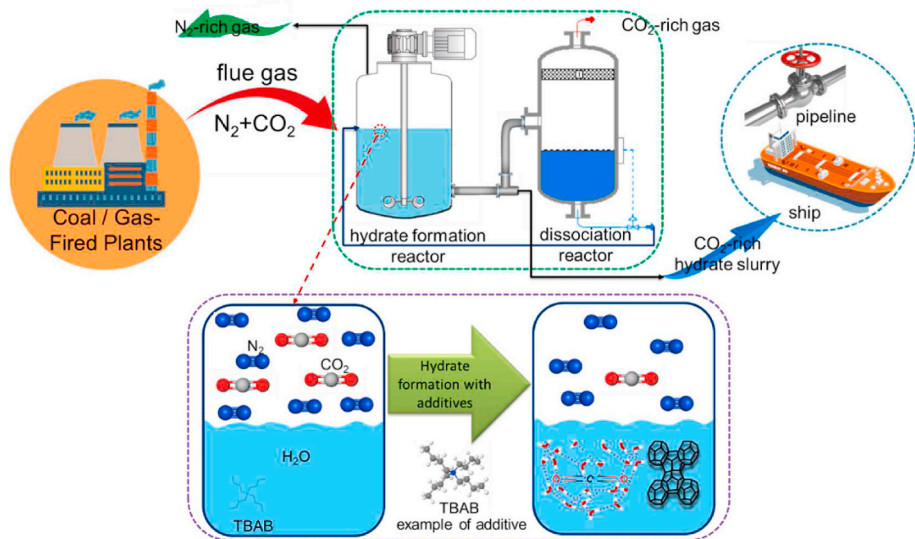


**Fig. 15.** Schematic process for hydrate-based CO<sub>2</sub> capture from flue gas.

[294] and molecular-scale spectroscopic features [295]. Nanobubbles have been investigated as an alternative approach, particularly in the context of natural gas hydrates [296]. These nanoscale gas-filled bubbles have the potential to enhance the nucleation process through heterogeneous mechanisms. Additionally, their presence can impact the selectivity of gas hydrates. Introducing hydrophobic and hydrophilic surfaces can also effectively facilitate nanobubble generation, leading to rapid hydrate formation [297–299]. However, the operational challenges associated with nanobubble hydrate systems have constrained the accuracy of this approach.

The significant challenge in the micro and meso-scale studies of CO<sub>2</sub> hydrates is due to the limitations of the current experimental and computational techniques. It is required to develop novel experiments, along with innovative computational models. To achieve this, multidisciplinary research collaborations are greatly important.

Enhancing the discussion on hydrate-based decarbonisation fundamentals with recent advancements delivers a clearer picture of the potential and challenges in hydrate-based CO<sub>2</sub> separation technologies. The addition of novel materials and methodologies offers promising paths to improve the efficiency and feasibility of CO<sub>2</sub> capture, a critical step toward sustainable environmental solutions.

A study by Liu et al. (2021) delved into the kinetics of the CO<sub>2</sub> hydrate formation in the presence of acid-dissolvable organic matters,

suggesting that the marine sediment's organic composition significantly influences CO<sub>2</sub> sequestration efficiency [300]. Moreover, the interaction between metal-organic frameworks (MOFs) and CO<sub>2</sub> gas hydrates heralds a transformative era for CO<sub>2</sub> capture and methane storage techniques [301]. MOFs, characterised by their large specific surface areas and pore sizes, present an unparalleled scaffold that significantly advances the thermodynamics and kinetics of CO<sub>2</sub> hydrate formation. This synergy expands the selection of materials within hydrate-based applications and highlights the fundamental role of rigorous research into MOF-CO<sub>2</sub> hydrate interactions. Such research could help develop more proficient CO<sub>2</sub> capture approaches and storage solutions. The attractive findings from studies on MOFs coupled with hydrates call for a concerted effort across scientific disciplines. This multidisciplinary approach is necessary to deepen our comprehension of these complex systems and to plan innovative and eco-friendly strategies for CO<sub>2</sub> management.

Additionally, leveraging the synergy between MOFs and hydrates, particularly for CH<sub>4</sub> storage, has showcased extensive potential, indicating an enhanced capacity for CH<sub>4</sub> containment under milder conditions compared to traditional methods [301]. The unique physicochemical properties of MOFs facilitate the formation of hydrates, thus increasing the volumetric and gravimetric storage densities. This harmonious integration of MOFs with gas hydrates lays the groundwork

for novel approaches that could revolutionise the energy sector. As global energy demands burgeon, these findings catalyse the hunt for sustainable energy practices, ensuring that CH<sub>4</sub>, a critical component of natural gas, is utilised efficiently and responsibly. The empirical evidence from various studies propels this field toward the threshold of innovation, where sustainable practices meet the escalating energy needs of tomorrow.

Expanding the understanding of material effects on CO<sub>2</sub> hydrate formation, Yan et al. (2018) assessed the role of graphene oxide (GO) nanoparticles, showcasing their efficacy in promoting CO<sub>2</sub> hydrate formation under varied temperature and pressure conditions [302]. The ability of GO nanoparticles to substantially moderate induction time and enhance gas consumption presents a novel method to improve the kinetics of hydrate formation, highlighting the importance of nanomaterials in developing competent CCS solutions.

Liu et al. (2022) investigated the carbonation behaviour of calcium silicate hydrate (C-S-H) [303], delivering a deeper understanding of C-S-H's potential for CO<sub>2</sub> capture through a detailed analysis of its carbonation kinetics and the evolution of carbonation products. The study highlights the role of environmental and material properties in influencing carbonation, offering insights into CO<sub>2</sub> sequestration using cementitious materials.

Addressing the role of saline conditions, Mok et al. (2023) investigated the NaCl-induced improvements in CO<sub>2</sub> selectivity during hydrate formation [304]. Their results highlight the nuanced impact of salts on both the thermodynamic and kinetic aspects of hydrate formation, emphasising the significance of considering saline water's influence on CO<sub>2</sub> sequestration strategies. The application of molecular dynamics simulations to study CO<sub>2</sub> hydrate growth in salt-containing electrolyte solutions by Wang et al. (2023) offered critical insights into how salt ions and thermodynamic conditions affect hydrate growth rates [305]. This study provides a fundamental understanding of seawater's CO<sub>2</sub> hydrate generation mechanism, guiding the future development of CO<sub>2</sub> sequestration technologies via hydrate formation in marine environments.

In rounding off the discussion on hydrate-based decarbonisation fundamentals, the potential of this technology stretches beyond current applications. Advances in understanding the microscopic and macroscopic mechanisms of hydrate formation hold the promise of optimising CO<sub>2</sub> capture processes to meet the constraints of environmental sustainability. As we continue exploring the complex dynamics of CO<sub>2</sub> and CH<sub>4</sub> hydrates, particularly in the presence of MOFs and other novel materials, bridging the gap between laboratory-scale research and large-scale applications is crucial. The challenge lies in translating these elaborate interactions and kinetic behaviours into commercially viable solutions that can contribute to global efforts to reduce carbon footprints. This interest is not just a scientific endeavour but a collaborative mission that calls for aligning research, industry, and policy-making to connect the full potential of hydrate-based technologies for a greener future.

#### 4.2. Hydrate-based decarbonisation scale-up

Scaling up hydrate-based decarbonisation from laboratory experiments to industrial-scale operations presents opportunities and challenges. The scale-up process involves both technical and economic challenges, such as the thermodynamic understanding of the process for operation at high pressure and low temperature and the equipment and energy cost. One of the critical opportunities lies in its energy efficiency compared to other CCS technologies. The moderate operating temperature and pressure in HBCC make this process a potentially cost-effective solution for large-scale industrial applications [306]. The challenges in scaling up HBCC processes can be categorised into four areas.

1. Technical challenges: gas hydrate formation requires precise control over temperature and pressure conditions. The main technical

challenge in this process is to maintain these thermodynamic conditions on a large scale [307]. Developing novel materials and processes that can facilitate hydrate formation under milder conditions is a crucial area of future research. For instance, using promoters or additives, such as surfactants, can lower the pressure and temperature requirements for hydrate formation [308,309]. The other technical challenge is the hydrates blockage in the equipment. Research is needed to develop effective anti-agglomerants and strategies for hydrate management to ensure the smooth operation of HBCC. Further, hydrate-forming performance in gas-dispersion reactors depends on gas dispersion quality and heat-discharge capacity, both of which can deteriorate with scale-up [310]. Stirred-tank reactors face a major scale-up disadvantage due to a significant increase in required stirrer-driving power. In contrast, multiple-tube reactors can be scaled up more efficiently by increasing the number of tubes or tube diameter without drastically increasing flow velocity [310]. However, these findings by Mori (2015) are based on simplified models and do not account for potential issues like wall fouling or hydrate crystal formation, which could obstruct operation.

2. Economic challenges: The cost of implementing and operating a HBCC process on a large scale still needs to be comprehensively investigated. However, the costs for this process are relatively high due to the need for specialised equipment and energy required to maintain the necessary conditions for hydrate formation [310]. More recent research points to promising improvements. For instance, Nguyen (2022) [311] and Rezaei (2022) [312] provide more optimistic projections. Nguyen (2022) estimates the cost of HBCC to be 20–40 US\$/tonnes of CO<sub>2</sub> avoided with an energy penalty of 15 %, making it potentially competitive with conventional absorption methods [311].
3. Efficiency Challenges: While HBCC demonstrates effectiveness on a small scale, it remains to be seen how efficient the process would be when scaled up [307]. Further research is necessary to ascertain the potential efficiency of large-scale operations.
4. Environmental Challenges: Although HBCC is a promising technology, there are concerns about the potential environmental impact of large-scale operations [313]. These concerns include the potential for CO<sub>2</sub> leaks and the effects on local ecosystems. This challenge will be applied to any other CCS process.

The design and optimisation of HBCC is also a critical area of research. This involves the development of mathematical models and simulation tools to predict hydrate behaviour and guide the design of efficient and robust systems. Integrating HBCC with other processes, such as power generation or industrial processes, can enhance its feasibility and efficiency. Research is needed to explore such integration opportunities and assess their technical and economic viability. In conclusion, the scale-up of HBCC is a complex and multifaceted process that requires research efforts linking science and engineering knowledge.

#### 4.3. Advances to promote the process of HBCC

Chemical additives/promoters can enhance the process of CO<sub>2</sub> separation in HBCC. Hydrate promoters can increase gas consumption and hydrate production rate [314]. They work by altering the thermodynamical conditions, allowing hydrate formation at lower pressures and higher temperatures [315]. Chemical methods use thermodynamic and kinetic additives like tetrahydrofuran (THF) [316], tetrabutylammonium bromide (TBAB) [317], and cyclopentane (CP) [318] to moderate phase equilibrium. TBAB has been highlighted as an eco-friendly additive that reduces energy consumption and boosts CO<sub>2</sub> hydration. The orthorhombic TBAB·38H<sub>2</sub>O·nCO<sub>2</sub> ionic clathrate is reported as the most effective lattice structure for CO<sub>2</sub> capture [319]. Kinetic additives such as sodium dodecyl sulfate (SDS), sodium dodecylbenzenesulfonate (SDBS), and cetyltrimethylammonium bromide (CTAB) are also

commonly employed [320,321]. Some additives have both thermodynamic and kinetic properties, i.e., 1,3-dioxolane (DIOX) shows the dual-action additive for the formation of hydrate [322,323]. Molecular dynamic simulation shows that promoters such as urea increases the CO<sub>2</sub> mass transfer and catalyses the cage formation [324]. Furthermore, some plants and fungi are reported to increase the kinetic formation of bio clathrate CO<sub>2</sub> [325].

Some non-ionic surfactants including Span80, Tween80, Span20 and Tween20 have also the ability to increase the hydrate growth rate [326]. They reduce the surface tension, promoting the dispersion of gas bubbles in the water phase [279]. This increases the contact area between the gas and water, facilitating the formation of hydrates and enhancing the efficiency of CO<sub>2</sub> separation.

Phan and Striolo (2023) employed molecular dynamics to study the effect of chemical additives, particularly aziridine, pyrrolidine, and THF, on CO<sub>2</sub> hydrate growth and dissociation [308]. They demonstrated that aziridine, while not reducing the nearly 30 wt% CO<sub>2</sub> storage capacity of the hydrates, outperformed the others in accelerating growth rates. Crucial to their findings was the correlation between the kinetics of CO<sub>2</sub> hydrate growth and factors such as the free energy barrier for CO<sub>2</sub> desorption and the binding energy of additives. The investigation also encompassed nitrogen-containing heterocyclic compounds at pressures of 25.5 bar and temperatures ranging from 269.1 to 289.1 K, where they showed promise as thermodynamic promoters. However, their effectiveness in shifting coexistence curves was less than THF. Mid-infrared (MIR) fiber-optic evanescent field sensing technique was also used to characterise IR absorption of some additives (e.g., THF and SDS) and their promoting effect [327]. Liu et al. (2023) investigated CO<sub>2</sub> capture by hydrates and reported that TBAB, CP, and THF enhance hydrate formation and CO<sub>2</sub> capture [328].

Hassan et al. (2020) investigated CO<sub>2</sub> hydrate formation in integrated gasification combined cycle (IGCC) conditions [329]. Using an isochoric system, they determined hydrate formation through CO<sub>2</sub> solubility in water. The study demonstrated increased CO<sub>2</sub> uptake with the expansion of ΔP, and combined promoter type T1-5 and T3-2 showed the best results, achieving 5.95 and 5.57 mmol of CO<sub>2</sub> per g of H<sub>2</sub>O, respectively.

The prevailing trend in the field is the combination of different chemical promoters for CO<sub>2</sub> hydrate formation, potentially offering a more effective and efficient approach to CO<sub>2</sub> capture. As a response to the increasing interest in leveraging chemical promoters for CO<sub>2</sub> hydrate, Wang et al. explored the idea of combining different promoters to capitalise on their varying functionalities [271]. They investigated the impact of 0.244 g L<sup>-1</sup> SDS, 0.288 g L<sup>-1</sup> TBAB, and 0.33 g L<sup>-1</sup> nano graphite, both individually and in combination. Among the combined systems, SDS-TBAB yielded the best-promoting effect. Zhang et al. focused on exploring the impact of anionic surfactant SDS and cationic surfactant dodecyltrimethylammonium chloride (DTAC) on the kinetics of CO<sub>2</sub>-TBAB hydrate formation, a crucial substance known for moderating CO<sub>2</sub> hydrate phase equilibrium but with a downside of decreasing CO<sub>2</sub> gas uptake [330]. The researchers utilised a batch reactor for conducting experiments with initial CO<sub>2</sub>/N<sub>2</sub> gas mixtures, using 10-wt% TBAB and varied SDS concentrations (0–1500 ppm) and DTAC concentrations (0–0.6 wt%). The study metrics included induction time, normalised gas uptake, split fraction, and separation factor. Results indicated that SDS accelerated hydrate formation most effectively, while DTAC showed superior CO<sub>2</sub> separation performance. The study concluded with the need for further research on the mechanism of the blockage effects and the role of surfactant micelles on the kinetics of CO<sub>2</sub>-TBAB hydrate formation.

The physical and chemical properties of the chemical additives is one the key important factors in CO<sub>2</sub> gas uptake during hydrate formation. For example, those additives with a strong polar ionic cause a formation of dense hydrate layer at the interface which results in decreasing of CO<sub>2</sub> gas diffusion and reducing CO<sub>2</sub> gas uptake [331]. On the other hand, the dissolution characteristics of weak polar or non-polar additives affect

the CO<sub>2</sub> gas uptake [331]. The liquid to the gas ration is also another factor in CO<sub>2</sub> gas uptake. It was demonstrated that the CO<sub>2</sub> storage capacity is maximised at 8.25 M liquid water–gas ratio which led to CO<sub>2</sub> gas uptake of ~9.1 L at standard condition [332].

One of the key mechanical methods used in HBCC is pressure control. By carefully controlling the pressure conditions under which hydrates form and dissociate, it is possible to optimise the CO<sub>2</sub> separation process. Temperature control is another critical mechanical method. Moreover, flow control is a critical aspect of HBCC. By controlling the flow rate of the gas and water, it is possible to optimise the contact between them, enhancing the formation of hydrates. Flow control can also help prevent the formation of large hydrate chunks that can cause blockage.

Mixing is a mechanical method that enhance the efficiency of HBCC. Mixing can be achieved through various means, such as agitation or static mixers. The mechanical method aims to enhance mass/heat transfer by introducing mechanical disturbances. However, conventional hydrate reactors like stirring [333], spraying [334], and bubbling reactors [335] could not meet the demands of large-scale hydrate formation and gas separation process. Some new reactor designs like a pilot-scale continuous jet hydrate reactor [336] and a high-speed spray device in the pipeline reactor [337] have been developed, aiming to enhance the gas–liquid interface and promote rapid formation of the gas hydrate. In a recent development, Xue (2023) conducted a study using a 15 L pilot-scale jet impingement stream reactor to separate CH<sub>4</sub> from CO<sub>2</sub> in biogas [338]. The reactor achieved a peak space velocity of 557 h<sup>-1</sup> and a maximum gas uptake of 1.00 mol L<sup>-1</sup> at 4.0 MPa. A CH<sub>4</sub> concentration of 50.0 % was increased to 70.0 % after the first stage of hydration separation and to 95.1 % after four-stage separation. CH<sub>4</sub> recovery rate and CO<sub>2</sub> capture ratio were found to be 58.8–78.2 % and 52.0–75.8 % in one stage, respectively.

While various mechanical methods have been used to enhance HBCC, there is still much room for improvement. Future research should focus on developing more efficient and reliable pressure, temperature, flow, and mixing control methods.

#### 4.4. From laboratory to industrial scale: a scale-up framework

Scale-up of HBCC from laboratory to industrial scale presents a unique set of challenges. One of the primary challenges is the energy consumption. The energy required for hydrate formation/dissociation can be substantial, especially at industrial levels. This energy demand can pose a significant challenge. Moreover, the energy used in the process, if derived from non-renewable sources, could contribute to the very problem the technology is trying to solve.

In a study by Rezaei (2022), HBCC was integrated with membrane separation and amine-absorption techniques to design hybrid CO<sub>2</sub>/H<sub>2</sub> separation processes [312]. The economic analysis, based on different flow rates and the application of various hydrate promoters, showed that combining hydrate formation and membrane separation resulted in the most cost-effective process, mainly when TBAB was used as a hydrate promoter. This combination resulted in a total cost of \$29.47 per ton of captured CO<sub>2</sub>. Despite the increase in energy consumption for hydrate formation when TBAB was used, its high separation efficiency significantly reduced the overall cost of the process.

Dashti and Lou (2018) developed a model for estimating energy requirements in different stages of HBCC, taking into account the influence of various chemical additives [339]. The application of this model demonstrated that chemical additives, specifically THF, substantially reduced the total energy consumption through impacts on CO<sub>2</sub> hydrate formation and dissociation pressures and temperatures, as well as hydration kinetics.

Recent research has shown significant advances in scaling up HBCC. As highlighted by Surovtseva et al. (2011), an innovative CO<sub>2</sub> capture technology applied to integrated gasification combined cycle (IGCC) power plants effectively combines cryogenic condensation and hydrate formation, significantly reducing CO<sub>2</sub> concentration from 75 mol% to 7

mol% in a two-stage process [340]. This method demonstrated considerable effectiveness as up to 80 mol% of CO<sub>2</sub> could be captured.

Dashti et al. (2021) established a foundational approach for large-scale implementation of the HBCC process through the development of reactor-scale models [341]. Two distinct models were developed: a basic model, which focuses on estimating the role of mass and heat transfer during the dissolution phase, and an improved model that incorporates both dissolution and hydrate formation processes. The improved model identifies mass transfer as the rate-controlling mechanism, a significant insight that influences reactor operation strategy. Moreover, comparing these two models highlighted the substantial impact of the consumption/reaction term on the reactor profiles, further emphasising the necessity of considering hydrate formation for realistic process simulation. Using time-dependent boundary conditions for the bulk gas, the improved model was successfully applied to batch operations and scaled up using parameters such as volume, time, and length.

Safe and efficient CO<sub>2</sub> storage is critical to any CCS technology, including HBCC. Developing and implementing effective storage solutions is a complex task involving considerations related to geology, engineering, safety, and regulation. Furthermore, the transition from laboratory to industrial scale often involves dealing with issues related to the handling and storing large volumes of CO<sub>2</sub>. Lastly, there are challenges related to integrating HBCC into existing industrial processes. These systems must be designed and operated to be compatible with existing infrastructure and operations. Despite these challenges, the potential benefits of HBCC make it a promising avenue for future research and development.

#### 4.5. Advantages and limitations of HBCC

HBCC presents a range of advantages, drawing attention to carbon sequestration technology. Foremost, it offers a higher storage density compared to conventional storage methods. One volume of hydrate structure can store approximately 160 vol of CO<sub>2</sub>. The technology also provides a safer storage medium as CO<sub>2</sub> hydrates are more stable than gaseous or supercritical states, reducing the risk of accidental leaks. HBCC has flexibility in application; it can be used on power plant flue gases, industrial emissions, and even direct air capture. Additionally, it potentially facilitates the CO<sub>2</sub> transportation via pipeline, a practice already employed for natural gas. Finally, gas hydrate technology may enable the use of CO<sub>2</sub> in enhanced oil recovery.

Despite these advantages, the widespread application of HBCC is hindered by significant challenges. One of the main challenges is the slow kinetics of hydrate formation and decomposition. In practice, this sluggishness in the kinetics can potentially hinder the time effectiveness of the process. The formation of hydrates requires specific conditions, which may be energy-intensive to maintain. Moreover, separating CO<sub>2</sub> from other flue gas constituents using hydrates is not sufficiently efficient, requiring additional stages of gas treatment such as scrubbing with amines to remove contaminants like SO<sub>2</sub> and NO<sub>x</sub>. The use of additives to promote hydrate formation is another concern, as these can have environmental implications. Lastly, the technology's readiness and commercial viability are still uncertain. The need for established large-scale demonstration projects for HBCC has resulted in a substantial shortage of data relevant to large-scale operation. As such, the economic assessments of this process mainly rely on theoretical or laboratory-scale studies.

#### CRediT authorship contribution statement

**Morteza Aminnaji:** Writing – review & editing, Writing – original draft, Validation, Supervision, Software, Methodology, Investigation, Formal analysis, Data curation, Conceptualization. **M Fahed Qureshi:** Writing – review & editing, Writing – original draft, Validation, Investigation, Formal analysis, Data curation. **Hossein Dashti:** Writing – review & editing, Writing – original draft, Validation, Investigation,

Formal analysis, Data curation. **Alfred Hase:** Writing – review & editing, Validation, Methodology, Conceptualization. **Abdolali Mosalanejad:** Writing – review & editing, Writing – original draft, Validation, Investigation, Formal analysis, Data curation. **Amir Jahanbakhsh:** Writing – review & editing, Writing – original draft, Validation, Investigation, Formal analysis, Data curation. **Masoud Babaei:** Writing – review & editing, Validation, Methodology, Conceptualization. **Amirpiran Amiri:** Writing – review & editing, Validation, Methodology, Conceptualization. **Mercedes Maroto-Valer:** Writing – review & editing, Validation, Methodology, Conceptualization.

#### Declaration of competing interest

The authors declare that they have no known competing financial interests or personal relationships that could have appeared to influence the work reported in this paper.

#### Data availability

Data will be made available on request.

#### Acknowledgements

A. Jahanbakhsh and M. M. Maroto-Valer would like to acknowledge that this work was supported by the UKRI ISCF Industrial Challenge within the UK Industrial Decarbonisation Research and Innovation Centre (IDRIC) award number: EP/V027050/1.

#### References

- [1] Friedlingstein P, Jones MW, O'sullivan M, Andrew RM, Hauck J, Peters GP, et al. Global carbon budget 2019. *Earth Syst Sci Data* 2019;11:1783–838.
- [2] Sikdar SK, Princiotta F. Advances in carbon management technologies. Boca Raton: CRC Press; 2020.
- [3] Prentice IC, Farquhar GD, Fasham MJR, Goulden ML, Heimann M, Jaramillo VJ, et al. The carbon cycle and atmospheric carbon dioxide. 2001.
- [4] Falkowski P, Scholes RJ, Boyle EEA, Canadell J, Canfield D, Elser J, et al. The global carbon cycle: a test of our knowledge of earth as a system. *Science* 2000;290:291–6.
- [5] Forster P, Ramaswamy V, Artaxo P, Berntsen T, Betts R, Fahey D W, Haywood J, Lean J, Lowe D C, Myhre G, Nganga J, Prinn R, Raga G, Schulz M, and Van Dorland R. Changes in Atmospheric Constituents and in Radiative Forcing. Chapter 2. United Kingdom: N. p., 2007. Web.
- [6] Dlugokencky EJ, Myers RC, Lang PM, Masarie KA, Crotwell AM, Thoning KW, et al. Conversion of NOAA atmospheric dry air CH<sub>4</sub> mole fractions to a gravimetrically prepared standard scale. *J Geophys Res Atmos* 2005;110.
- [7] Etheridge DM, Steele LP, Langenfelds RL, Francey RJ, Barnola J-M, Morgan VI. Natural and anthropogenic changes in atmospheric CO<sub>2</sub> over the last 1000 years from air in Antarctic ice and firn. *J Geophys Res Atmos* 1996;101:4115–28.
- [8] Hansen J, Ruedy R, Sato M, Lo K. Global surface temperature change. *Rev Geophys* 2010;48.
- [9] Vooradi R, Bertran M-O, Frauzem R, Anne SB, Gani R. Sustainable chemical processing and energy-carbon dioxide management: review of challenges and opportunities. *Chem Eng Res Des* 2018;131:440–64.
- [10] Liddle B, Sadorsky P. How much does increasing non-fossil fuels in electricity generation reduce carbon dioxide emissions? *Appl Energy* 2017;197:212–21.
- [11] Keeling CD, Whorf TP, Wahlen M, der Plicht J. Interannual extremes in the rate of rise of atmospheric carbon dioxide since 1980. *Nature* 1995;375:666–70.
- [12] Raupach MR, Marland G, Ciais P, Le Quéré C, Canadell JG, Klepper G, et al. Global and regional drivers of accelerating CO<sub>2</sub> emissions. *Proc Natl Acad Sci USA* 2007;104:10288–93.
- [13] Warren R. The role of interactions in a world implementing adaptation and mitigation solutions to climate change. *Philos Trans R Soc A Math Phys Eng Sci* 2011;369:217–41.
- [14] Doney SC, Fabry VJ, Feely RA, Kleypas JA. Ocean acidification: the other CO<sub>2</sub> problem. *Ann Rev Mar Sci* 2009;1:169–92.
- [15]Gattuso J-P, Hansson L. Ocean acidification. Oxford university press; 2011.
- [16] Guinotte JM, Fabry VJ. Ocean acidification and its potential effects on marine ecosystems. *Ann N Y Acad Sci* 2008;1134:320–42.
- [17] Hare B, Schaeffer M, Rocha M. Science aspects of the 2 C and 1.5 C global goals in the Cancun Agreements. LDC Pap Ser 2011. <https://www.ldc-climate.org/wp-content/uploads/2018/02/LDC-paper-series-22.pdf>.
- [18] Sloan ED. Fundamental principles and applications of natural gas hydrates. *Nature* 2003;426:353–63.
- [19] Sloan ED, Koh CA. Clathrate hydrates of natural gases third edition, vol. 119. Chem Ind YORK THEN BOCA RATON-MARCEL DEKKER THEN CRC Press; 2008.

- [20] Koh CA. Towards a fundamental understanding of natural gas hydrates. *Chem Soc Rev* 2002;31:157–67.
- [21] Gabitto JF, Tsouris C. Physical properties of gas hydrates: a review. *J Thermodyn* 2010;2010.
- [22] Ripmeester JA, John ST, Ratcliffe CI, Powell BM. A new clathrate hydrate structure. *Nature* 1987;325:135–6.
- [23] Ripmeester JA, Ratcliffe CI. Xenon-129 NMR studies of clathrate hydrates: new guests for structure II and structure H. *J Phys Chem* 1990;94:8773–6.
- [24] Mehta AP, Sloan Jr ED. Structure H hydrate phase equilibria of paraffins, naphthenes, and olefins with methane, vol. 39. *J Chem Eng Data*; 1994. p. 887–90.
- [25] Chou I-M, Sharma A, Burruss RC, Shu J, Mao H, Hemley RJ, et al. Transformations in methane hydrates. *Proc Natl Acad Sci USA* 2000;97:13484–7.
- [26] Shu J, Chen X, Chou I-M, Yang W, Hu J, Hemley RJ, et al. Structural stability of methane hydrate at high pressures. *Geosci Front* 2011;2:93–100.
- [27] Takeya S, Kamata Y, Uchida T, Nagao J, Ebinuma T, Narita H, et al. Coexistence of structure I and II hydrates formed from a mixture of methane and ethane gases. *Can J Phys* 2003;81:479–84.
- [28] Pang J, Liang Y, Masuda Y, Takeya S. Structural transition of the methane–ethane mixture hydrate in a hydrate/water/hydrocarbon three-phase coexistence system: effect of gas concentration. *ACS Sustain Chem & Eng* 2020;8:16924–37.
- [29] Stoporev AS, Ogienko AG, Sizikov AA, Semenov AP, Kopitsyn DS, Vinokurov VA, et al. Unexpected formation of sII methane hydrate in some water-in-oil emulsions: different reasons for the same phenomenon. *J Nat Gas Sci Eng* 2018;60:284–93.
- [30] Aminnaji M, Anderson R, Tohidi B. Experimental measurement of multiple hydrate structure formation in binary and ternary natural gas analogue systems by isochoric equilibrium methods. *Energy & Fuels* 2023;35:9341–8. <https://doi.org/10.1021/acs.energyfuels.1c00792>.
- [31] Aminnaji M, Anderson R, Tohidi B. Anomalous KHI-Induced dissociation of gas hydrates inside the hydrate stability zone: experimental observations & potential mechanisms. *J Pet Sci Eng* 2019;178:1044–50.
- [32] Aminnaji M, Hase A, Crombie L. Anti-agglomerants: study of hydrate structural, gas composition, hydrate amount, and water cut effect. *Int Pet Technol Conf* 2023. <https://doi.org/10.2523/IPTC-22765-MS>. OnePetro.
- [33] Anderson R, Aminnaji M, Kalorazi BT. Effect of Gas Composition on Hydrate Growth Rate and Agglomeration Tendency. <https://researchportal.hw.ac.uk/en/publications/effect-of-gas-composition-on-hydrate-growth-rate-and-aggro-meratio>.
- [34] Pan M, Lutz-Helbing M, Schicks JM. Heterogeneous and coexisting hydrate Phases—formation under natural and laboratory conditions. *Energy & Fuels* 2022;36:10489–503. <https://doi.org/10.1021/ACS.ENERGYFUELS.2C01326>.
- [35] Sakamoto H, Sato K, Shiraiwa K, Takeya S, Nakajima M, Ohmura R. Synthesis, characterization and thermal-property measurements of ionic semi-clathrate hydrates formed with tetrabutylphosphonium chloride and tetrabutylammonium acrylate. *RSC Adv* 2011;1:315–22.
- [36] Suginaka T, Sakamoto H, Iino K, Takeya S, Nakajima M, Ohmura R. Thermodynamic properties of ionic semiclathrate hydrate formed with tetrabutylphosphonium bromide. *Fluid Phase Equilib* 2012;317:25–8.
- [37] Darbouret M, Cournil M, Herri J-M. Rheological study of TBAB hydrate slurries as secondary two-phase refrigerants. *Int J Refrig* 2005;28:663–71.
- [38] Douzet J, Kwaterski M, Lallemand A, Chauvy F, Flick D, Herri J-M. Prototyping of a real size air-conditioning system using a tetra-n-butylammonium bromide semi-clathrate hydrate slurry as secondary two-phase refrigerant—Experimental investigations and modelling. *Int J Refrig* 2013;36:1616–31.
- [39] Hashimoto H, Yamaguchi T, Kinoshita T, Muromachi S. Gas separation of flue gas by tetra-n-butylammonium bromide hydrates under moderate pressure conditions. *Energy* 2017;129:292–8.
- [40] Hashimoto H, Yamaguchi T, Ozeki H, Muromachi S. Structure-driven CO<sub>2</sub> selectivity and gas capacity of ionic clathrate hydrates. *Sci Rep* 2017;7:1–10.
- [41] Chapoy A, Anderson R, Tohidi B. Low-pressure molecular hydrogen storage in semi-clathrate hydrates of quaternary ammonium compounds. *J Am Chem Soc* 2007;129:746–7.
- [42] Arjmandi M, Chapoy A, Tohidi B. Equilibrium data of hydrogen, methane, nitrogen, carbon dioxide, and natural gas in semi-clathrate hydrates of tetrabutyl ammonium bromide. *J Chem & Eng Data* 2007;52:2153–8.
- [43] Yin Z, Zheng J, Kim H, Seo Y, Linga P. Hydrates for cold energy storage and transport: a review. *Adv Appl Energy* 2021;2:100022.
- [44] Kim H, Zheng J, Yin Z, Kumar S, Tee J, Seo Y, et al. An electrical resistivity-based method for measuring semi-clathrate hydrate formation kinetics: application for cold storage and transport. *Appl Energy* 2022;308:118397.
- [45] Khafei A, Kamran-Pirzaman A. Experimental study of semiclathrate hydrates formation TBAOH, TBAF, and TBAC in the presence of SDS and tween surfactants as a cold thermal energy storage system for air conditioning applications. *J Chem & Eng Data* 2021;66:2901–10.
- [46] Sugahara T, Machida H, Muromachi S, Tenma N. Thermodynamic properties of tetra-n-butylammonium 2-ethylbutyrate semiclathrate hydrate for latent heat storage. *Int J Refrig* 2019;106:113–9.
- [47] Muromachi S, Takeya S. Gas-containing semiclathrate hydrate formation by tetra-n-butylammonium carboxylates: acrylate and butyrate. *Fluid Phase Equilib* 2017;441:59–63.
- [48] Shimada J, Shimada M, Sugahara T, Tsunashima K, Tani A, Tsuchida Y, et al. Phase equilibrium relations of semiclathrate hydrates based on tetra-n-butylphosphonium formate, acetate, and lactate. *J Chem & Eng Data* 2018;63:3615–20.
- [49] Muromachi S, Takeya S. Thermodynamic properties and crystallographic characterization of semiclathrate hydrates formed with tetra-n-butylammonium glycolate. *ACS Omega* 2019;4:7317–22.
- [50] Oshima M, Kida M, Jin Y, Nagao J. Dissociation behaviour of (tetra-n-butylammonium bromide+ tetra-n-butylammonium chloride) mixed semiclathrate hydrate systems. *J Chem Thermodyn* 2015;90:277–81.
- [51] Iwai T, Miyamoto T, Kurokawa N, Hotta A, Ohmura R. Synthesis and evaluation of green phase change materials for efficient air conditioning by tetrabutylphosphonium phosphate ionic semiclathrate hydrate. *J Energy Storage* 2022;52:104801.
- [52] Davidson DW. Water: a comprehensive treatise. *Clathrate Hydrates* 1973;2:115–234.
- [53] Lipkowski J, Suwinska K, Rodionova TV, Udachin KA, Dyadin YA. Phase and X-ray study of clathrate formation in the tetraisoamylammonium fluoride-water system. *J Incl Phenom Mol Recognit Chem* 1994;17:137–48.
- [54] Koyama R, Hotta A, Ohmura R. Equilibrium temperature and dissociation heat of tetrabutylphosphonium acrylate (TBPAc) ionic semi-clathrate hydrate as a medium for the hydrate-based thermal energy storage system. *J Chem Thermodyn* 2020;144:106088.
- [55] Shimada J, Shimada M, Sugahara T, Tsunashima K. Phase equilibrium relations of tetra-n-butylphosphonium propionate and butyrate semiclathrate hydrates. *Fluid Phase Equilib* 2019;485:61–6.
- [56] Yamauchi Y, Yamasaki T, Endo F, Hotta A, Ohmura R. Thermodynamic properties of ionic semiclathrate hydrate formed with tetrabutylammonium propionate. *Chem Eng & Technol* 2017;40:1810–6.
- [57] Shimada J, Yamada M, Tani A, Sugahara T, Tsunashima K, Tsuchida Y, et al. Thermodynamic properties of tetra-n-butylphosphonium dicarboxylate semiclathrate hydrates. *J Chem & Eng Data* 2021;67:67–73.
- [58] Miyamoto T, Koyama R, Kurokawa N, Hotta A, Alavi S, Ohmura R. Thermophysical property measurements of tetrabutylphosphonium oxalate (TBPOx) ionic semiclathrate hydrate as a media for the thermal energy storage system. *Front Chem* 2020;8:547.
- [59] Muromachi S, Takeya S, Alavi S, Ripmeester JA. Structural CO<sub>2</sub> capture preference of semiclathrate hydrate formed with tetra-n-butylammonium chloride. *CrystEngComm* 2022;24:4366–71. <https://doi.org/10.1039/DCE00598K>.
- [60] Shimada W, Shiro M, Kondo H, Takeya S, Oyama H, Ebinuma T, et al. Tetra-n-butylammonium bromide-water (1/38). *Acta Crystallogr Sect C Cryst Struct Commun* 2005;61:o65–6.
- [61] Muromachi S, Takeya S, Yamamoto Y, Ohmura R. Characterization of tetra-n-butylphosphonium bromide semiclathrate hydrate by crystal structure analysis. *CrystEngComm* 2014;16:2056–60.
- [62] Shimada W, Ebinuma T, Oyama H, Kamata Y, Takeya S, Uchida T, et al. Separation of gas molecule using tetra-n-butyl ammonium bromide semi-clathrate hydrate crystals. *Jpn J Appl Phys* 2003;42:L129.
- [63] Wang X, Dennis M. Phase equilibrium and formation behaviour of CO<sub>2</sub>-TBAB semi-clathrate hydrate at low pressures for cold storage air conditioning applications. *Chem Eng Sci* 2016;155:294–305.
- [64] Deschamps J, Dalmazzone D. Hydrogen storage in semiclathrate hydrates of tetrabutyl ammonium chloride and tetrabutyl phosphonium bromide. *J Chem & Eng Data* 2010;55:3395–9.
- [65] Mohammadi AH, Richon D. Phase equilibria of semi-clathrate hydrates of tetra-n-butylammonium bromide+ hydrogen sulfide and tetra-n-butylammonium bromide+ methane. *J Chem & Eng Data* 2010;55:982–4.
- [66] Hassan H, Zebarast S, Gandomkar M. A new highly stable methane hydrate from the synergic mixture of common promoters: experimental and modeling surveys. *J Nat Gas Sci Eng* 2021;93:104056.
- [67] Renault-Crispo J-S, Servio P. Methane gas hydrate kinetics with mixtures of sodium dodecyl sulphate and tetrabutylammonium bromide. *Can J Chem Eng* 2018;96:1620–6.
- [68] Oyama H, Ebinuma T, Nagao J, Narita H, Shimada W. Phase behavior of TBAB semiclathrate hydrate crystal under several vapor components. 2008.
- [69] Baghban A, Ahmadi MA, Pouladi B, Amanna B. Phase equilibrium modeling of semi-clathrate hydrates of seven commonly gases in the presence of TBAB ionic liquid promoter based on a low parameter connectionist technique. *J Supercrit Fluids* 2015;101:184–92.
- [70] Tzirakis F, Stringari P, Von Solms N, Coquelet C, Kontogeorgis G. Hydrate equilibrium data for the CO<sub>2</sub>+ N<sub>2</sub> system with the use of tetra-n-butylammonium bromide (TBAB), cyclopentane (CP) and their mixture. *Fluid Phase Equilib* 2016;408:240–7.
- [71] Godishala KK, Sangwai JS, Sami NA, Das K. Phase stability of semiclathrate hydrates of carbon dioxide in synthetic sea water. *J Chem & Eng Data* 2013;58:1062–7.
- [72] Hassan H, Pahlavanzadeh H. Thermodynamic modeling and experimental measurement of semi-clathrate hydrate phase equilibria for CH<sub>4</sub> in the presence of cyclohexane (CH) and tetra-n-butyl ammonium bromide (TBAB) mixture. *J Nat Gas Sci Eng* 2020;75:103128.
- [73] Shi L, Yi L, Shen X, Wu W, Liang D. Dissociation temperatures of mixed semiclathrate hydrates formed with tetrabutylammonium bromide plus tetrabutylammonium chloride. *J Chem & Eng Data* 2016;61:2155–9.
- [74] Lee S, Park S, Lee Y, Lee J, Lee H, Seo Y. Guest gas enclathration in semiclathrates of tetra-n-butylammonium bromide: stability condition and spectroscopic analysis. *Langmuir* 2011;27:10597–603.
- [75] Imai S, Okutani K, Ohmura R, Mori YH. Phase equilibrium for clathrate hydrates formed with difluoromethane+ either cyclopentane or tetra-n-butylammonium bromide. *J Chem & Eng Data* 2005;50:1783–6.

- [76] Chua PC, Kelland MA. Tetra (iso-hexyl) ammonium bromide- the most powerful quaternary ammonium-based tetrahydrofuran crystal growth inhibitor and synergist with polyvinylcaprolactam kinetic gas hydrate inhibitor. *Energy & Fuels* 2012;26:1160–8.
- [77] Hussain HH, Husin H. Review on application of quaternary ammonium salts for gas hydrate inhibition. *Appl Sci* 2020;10:1011.
- [78] Nguyen NN, Nguyen AV, Nguyen KT, Rintoul L, Dang LX. Unexpected inhibition of CO<sub>2</sub> gas hydrate formation in dilute TBAB solutions and the critical role of interfacial water structure. *Fuel* 2016;185:517–23.
- [79] Pickering SUX. The hydrate theory of solutions. Some compounds of the alkylamines and ammonia with water. *J Chem Soc Trans* 1893;63:141–95.
- [80] Gregory MD. Hydration of several aliphatic amines in some Non-polar solvents. A dielectric study of aliphatic amine hydrates. The University of Oklahoma; 1968.
- [81] Jeffrey GA. Hydrate inclusion compounds. *J Incl Phenom* 1984;1:211–22.
- [82] Ogata K, Tsuda T, Amano S, Hashimoto S, Sugahara T, Ohgaki K. Hydrogen storage in trimethylamine hydrate: thermodynamic stability and hydrogen storage capacity of hydrogen+ trimethylamine mixed semi-clathrate hydrate. *Chem Eng Sci* 2010;65:1616–20.
- [83] McMullan RK, Jeffrey GA, Jordan TH. Polyhedral clathrate hydrates. XIV. The structure of (CH<sub>3</sub>)<sub>3</sub>CNH<sub>2</sub>·9/3·4H<sub>2</sub>O. *J Chem Phys* 1967;47:1229–34.
- [84] Youn Y, Cha M, Lee H. Structural transition of trimethylamine semi-hydrate by methane inclusion. *Fluid Phase Equilib* 2016;413:123–8.
- [85] Park S, Kang H, Shin K, Seo Y, Lee H. Structural transformation and tuning behavior induced by the propylamine concentration in hydrogen clathrate hydrates. *Phys Chem Chem Phys* 2015;17:1949–56.
- [86] Lee S, Lee Y, Park S, Seo Y. Structural transformation of isopropylamine semiclathrate hydrates in the presence of methane as a coguest. *J Phys Chem B* 2012;116:13476–80.
- [87] Cha M. Structural transition of trimethylamine hydrate by methane or hydrogen inclusion. *EGU Gen. Assem. Conf. Abstr.*; 2020. p. 3806.
- [88] Sahu C, Sircar A, Sangwai JS, Kumar R. Effect of methylamine, aminylamine, and decylamine on the formation and dissociation kinetics of CO<sub>2</sub> hydrate relevant for carbon dioxide sequestration. *Ind & Eng Chem Res* 2022;61:2672–8.
- [89] Udashin KA, Ratcliffe CI, Ripmeester JA. Structure, composition, and thermal expansion of CO<sub>2</sub> hydrate from single crystal X-ray diffraction measurements. *J Phys Chem B* 2001;105:4200–4.
- [90] Takeya S, Udashin KA, Moudrakovski IL, Susilo R, Ripmeester JA. Direct space methods for powder X-ray diffraction for guest-host materials: applications to cage occupancies and guest distributions in clathrate hydrates. <https://doi.org/10.1021/ja905426e>; 2022.
- [91] Takeya S, Miromachi S, Yamamoto Y, Umeda H, Matsuo S. Preservation of CO<sub>2</sub> hydrate under different atmospheric conditions. *Fluid Phase Equilib* 2016;413: 137–41. <https://doi.org/10.1016/j.fluid.2015.10.036>.
- [92] Ripmeester JA, Ratcliffe CI. The diverse nature of dodecahedral cages in clathrate hydrates as revealed by 129Xe and 13C NMR spectroscopy: CO<sub>2</sub> as a small-cage guest. *Energy & Fuels* 1998;12:197–200.
- [93] Henning RW, Schultz AJ, Thieu V, Halpern Y. Neutron diffraction studies of CO<sub>2</sub> clathrate hydrate: formation from deuterated ice. *J Phys Chem A* 2000;104: 5066–71.
- [94] Wf K, Chazallon B, Klapproth A, Pauer F. Filling-isotherms in clathrate-hydrates. *Rev High Press Sci Technol* 1998;7:1147–9.
- [95] Fleyfel F, Devlin JP. FT-IR spectra of 90 K films of simple, mixed, and double clathrate hydrates of trimethylene oxide, methyl chloride, carbon dioxide, tetrahydrofuran, and ethylene oxide containing decoupled water-d2. *J Phys Chem* 1988;92:631–5.
- [96] Chen L, Lu H, Ripmeester JA. Raman spectroscopic study of CO<sub>2</sub> in hydrate cages. *Chem Eng Sci* 2015;138:706–11. <https://doi.org/10.1016/J.CES.2015.09.001>.
- [97] Qin J, Kuhs WF. Quantitative analysis of gas hydrates using Raman spectroscopy. *AIChE J* 2013;59:2155–67. <https://doi.org/10.1002/AIC.13994>.
- [98] Pérez-Rodríguez M, Vidal-Vidal A, Rodríguez JM, Blas FJ, Torré J-P, Piñeiro MM. Computational study of the interplay between intermolecular interactions and CO<sub>2</sub> orientations in type I hydrates. *Phys Chem Chem Phys* 2017;19:3384–93.
- [99] Anderson GK. Enthalpy of dissociation and hydration number of carbon dioxide hydrate from the Clapeyron equation. *J Chem Thermodyn* 2003;35:1171–83. [https://doi.org/10.1016/S0021-9614\(03\)00093-4](https://doi.org/10.1016/S0021-9614(03)00093-4).
- [100] Vlahakis JG. The Growth Rate of Ice Crystals: the Properties of carbon dioxide hydrate; a review of properties of 51 gas hydrates. *OSW* 1972;830:14.
- [101] Sun R, Duan Z. Prediction of CH<sub>4</sub> and CO<sub>2</sub> hydrate phase equilibrium and cage occupancy from ab initio intermolecular potentials. *Geochim Cosmochim Acta* 2005;69:4411–24. <https://doi.org/10.1016/J.GCA.2005.05.012>.
- [102] Yoon JH, Yamamoto Y, Komai T, Haneda H, Kawamura T. Rigorous approach to the prediction of the heat of dissociation of gas hydrates. *Ind Eng Chem Res* 2003; 42:1111–4. <https://doi.org/10.1021/IE020598E>.
- [103] Staykova DK, Kuhs WF, Salamatian AN, Hansen T. Formation of porous gas hydrates from ice powders: diffraction experiments and multistage model. *J Phys Chem B* 2003;107:10299–311.
- [104] Prasad PSR, Shiva Prasad K, Thakur NK. FTIR signatures of type-II clathrates of carbon dioxide in natural quartz veins. *Curr Sci* 2006;90:1544–7.
- [105] Hester KC, Sloan ED. sI structural transitions from binary mixtures of simple sI formers. *Int J Thermophys* 2005;26:95–106.
- [106] Chen GJ, Guo TM. A new approach to gas hydrate modelling. *Chem Eng J* 1998; 71:145–51. [https://doi.org/10.1016/S1385-8947\(98\)00126-0](https://doi.org/10.1016/S1385-8947(98)00126-0).
- [107] Hashimoto S, Murayama S, Sugahara T, Ohgaki K. Phase equilibria for H<sub>2</sub> + CO<sub>2</sub> + tetrahydrofuran + water mixtures containing gas hydrates. *J Chem Eng Data* 2006;51:1884–6. <https://doi.org/10.1021/JE0602364>.
- [108] Belosludov VR, Bozhko YY, Subbotin OS, Belosludov RV, Zhdanov RK, Gets KV, et al. Influence of N<sub>2</sub> on formation conditions and guest distribution of mixed CO<sub>2</sub> + CH<sub>4</sub> gas hydrates. *Mol* 2018;23:3336. <https://doi.org/10.3390/MOLECULES23123336>. 2018;23:3336.
- [109] Zhong DL, Li Z, Lu YY, Sun DJ. Phase equilibrium data of gas hydrates formed from a CO<sub>2</sub> + CH<sub>4</sub> gas mixture in the presence of tetrahydrofuran. *J Chem Eng Data* 2014;59:4110–7. <https://doi.org/10.1021/JE500748Z>.
- [110] Lee YJ, Kawamura T, Yamamoto Y, Yoon JH. Phase equilibrium studies of tetrahydrofuran (THF) + CH<sub>4</sub>, THF + CO<sub>2</sub>, CH<sub>4</sub> + CO<sub>2</sub>, and THF + CO<sub>2</sub> + CH<sub>4</sub> hydrates. *J Chem Eng Data* 2012;57:3543–8. <https://doi.org/10.1021/ JE300850Q>.
- [111] Herslund PJ, Thomsen K, Abildskov J, Von Solms N. Phase equilibrium modeling of gas hydrate systems for CO<sub>2</sub> capture. *J Chem Thermodyn* 2012;48:13–27. <https://doi.org/10.1016/j.jct.2011.12.039>.
- [112] Uchida T, Ohmura R, Ikeda IY, Nagao J, Takeya S, Hori A. Phase equilibrium measurements and crystallographic analyses on structure-H type gas hydrate formed from the CH<sub>4</sub>-CO<sub>2</sub>-neohexane-water system. *J Phys Chem B* 2006;110: 4583–8. <https://doi.org/10.1021/JP056503E>.
- [113] Lee Y, Seo Y, Ahn T, Lee J, Lee JY, Kim S-J, et al. CH<sub>4</sub>-Flue gas replacement occurring in sH hydrates and its significance for CH<sub>4</sub> recovery and CO<sub>2</sub> sequestration. *Chem Eng J* 2017;308:50–8.
- [114] Lee Y, Lee D, Lee JW, Seo Y. Enclathration of CO<sub>2</sub> as a co-guest of structure H hydrates and its implications for CO<sub>2</sub> capture and sequestration. *Appl Energy* 2016;163:51–9. <https://doi.org/10.1016/J.APENERGY.2015.11.009>.
- [115] Lee D, Lee Y, Lim J, Seo Y. Guest enclathration and structural transition in CO<sub>2</sub> + N<sub>2</sub> + methylcyclopentane hydrates and their significance for CO<sub>2</sub> capture and sequestration. *Chem Eng J* 2017;320:43–9. <https://doi.org/10.1016/J.CEJ.2017.03.019>.
- [116] Zheng JN, Yang M, Chen B, Song Y, Wang D. Research on the CO<sub>2</sub> gas uptake of different hydrate structures with cyclopentane or methyl-cyclopentane as Co-guest molecules. *Energy Procedia* 2017;105:4133–9. <https://doi.org/10.1016/J.EGYPRO.2017.03.877>.
- [117] Zheng J-N, Yang M. Phase equilibrium data of CO<sub>2</sub> – MCP hydrates and CO<sub>2</sub> gas uptake comparisons with CO<sub>2</sub> – CP hydrates and CO<sub>2</sub> – C<sub>3</sub>H<sub>8</sub> hydrates. 2018. <https://doi.org/10.1021/acs.jced.8b00893>.
- [118] Choi W, Lee Y, Mol J, Seo Y. Influence of feed gas composition on structural transformation and guest exchange behaviors in sH hydrate – flue gas replacement for energy recovery and CO<sub>2</sub> sequestration. *Energy* 2020;207: 118299. <https://doi.org/10.1016/J.ENERGY.2020.118299>.
- [119] Lee Y, Moon S, Hong S, Lee S, Park Y. Observation of distinct structural transformation between sI and sH gas hydrates and their kinetic properties during CO<sub>2</sub> capture from N<sub>2</sub> + CO<sub>2</sub>. *Chem Eng J* 2020;389:123749. <https://doi.org/10.1016/J.CEJ.2019.123749>.
- [120] Tezuka K, Shen R, Watanabe T, Takeya S, Alavi S, Ripmeester JA, et al. Synthesis and characterization of a structure H hydrate formed with carbon dioxide and 3,3-dimethyl-2-butanone. *Chem Commun* 2012;49:505–7. <https://doi.org/10.1039/C2CC37717A>.
- [121] Joon Shin H, Lee YJ, Im JH, Won Han K, Lee JW, Lee Y, et al. Thermodynamic stability, spectroscopic identification and cage occupation of binary CO<sub>2</sub> clathrate hydrates. *Chem Eng Sci* 2009;64:5125–30. <https://doi.org/10.1016/J.CES.2009.08.019>.
- [122] Servio P, Lagers F, Peters C, Englezos P. Gas hydrate phase equilibrium in the system methane–carbon dioxide–neohexane and water. *Fluid Phase Equilib* 1999; 158–160:795–800. [https://doi.org/10.1016/S0378-3812\(99\)00084-9](https://doi.org/10.1016/S0378-3812(99)00084-9).
- [123] Lee Y, Kim Y, Seo Y. Enhanced CH<sub>4</sub> recovery induced via structural transformation in the CH<sub>4</sub>/CO<sub>2</sub> replacement that occurs in sH hydrates. *Environ Sci Technol* 2015;49:8899–906. [https://doi.org/10.1021/ACS.EST.5B01640/SUPPL\\_FILE/ES5B01640\\_SI\\_001.PDF](https://doi.org/10.1021/ACS.EST.5B01640/SUPPL_FILE/ES5B01640_SI_001.PDF).
- [124] Mohammadi AH, Esilamianesh A, Belandria V, Richon D. Phase equilibria of semiclathrate hydrates of CO<sub>2</sub>, N<sub>2</sub>, CH<sub>4</sub>, or H<sub>2</sub> + tetra-n-butylammonium bromide aqueous solution. *J Chem Eng Data* 2011;56:3855–65. <https://doi.org/10.1021/JE2005159>.
- [125] Duc NH, Chauvy F, Herri JM. CO<sub>2</sub> capture by hydrate crystallization – a potential solution for gas emission of steelmaking industry. *Energy Convers Manag* 2007; 48:1313–22. <https://doi.org/10.1016/J.ENCONMAN.2006.09.024>.
- [126] Momeni K, Jomekian A, Bazooray B. Semi-clathrate hydrate phase equilibria of carbon dioxide in presence of tetra-n-butyl-ammonium chloride (TBAC): experimental measurements and thermodynamic modeling. *Fluid Phase Equilib* 2020;508:112445. <https://doi.org/10.1016/J.FLUID.2019.112445>.
- [127] Sun ZG, Jiao LJ, Zhao ZG, Wang GL, Huang HF. Phase equilibrium conditions of semi-clathrate hydrates of (tetra-n-butyl ammonium chloride + carbon dioxide). *J Chem Thermodyn* 2014;75:116–8. <https://doi.org/10.1016/J.JCT.2014.02.020>.
- [128] Komatsu H, Ota M, Sato Y, Watanabe M, Smith RL. Hydrogen and carbon dioxide adsorption with tetra-n-butyl ammonium semi-clathrate hydrates for gas separations. *AIChE J* 2015;61:992–1003. <https://doi.org/10.1002/AIC.14689>.
- [129] Mesbar M, Abouali Galedari S, Soroush E, Momeni M. Modeling phase behavior of semi-clathrate hydrates of CO<sub>2</sub>, CH<sub>4</sub>, and N<sub>2</sub> in aqueous solution of tetra-n-butyl ammonium fluoride. *J Non-Equilibrium Thermodyn* 2019;44:155–67. <https://doi.org/10.1015/JNET-2018-0079/MACHINEREADABLECITATION/RIS>.
- [130] Sen Li X, Zhan H, Xu CG, Zeng ZY, Lv QN, Yan KF. Effects of tetrabutyl-(ammonium/phosphonium) salts on clathrate hydrate capture of CO<sub>2</sub> from simulated flue gas. *Energy and Fuels* 2012;26:2518–27. <https://doi.org/10.1021/EF3000399>.
- [131] Ilani-Kashkouli P, Mohammadi AH, Naidoo P, Ramjugernath D. Thermodynamic stability conditions for semi-clathrate hydrates of CO<sub>2</sub>, CH<sub>4</sub>, or N<sub>2</sub> with

- tetrabutyl ammonium nitrate (TBANO<sub>3</sub>) aqueous solution. *J Chem Thermodyn* 2016;96:52–6. <https://doi.org/10.1016/J.JCT.2015.11.030>.
- [132] Mayoufi N, Dalmazzzone D, Fürst W, Delahaye A, Fournaison L. CO<sub>2</sub> enclathration in hydrates of peralkyl-(Ammonium/Phosphonium) salts: stability conditions and dissociation enthalpies. *J Chem Eng Data* 2010;55:1271–5. <https://doi.org/10.1021/JE9006212>.
- [133] Sales Silva LP, Dalmazzzone D, Stambouli M, Lesort AL, Arpentinier P, Trueba A, et al. Phase equilibria of semi-clathrate hydrates of tetra-n-butyl phosphonium bromide at atmospheric pressure and in presence of CH<sub>4</sub> and CO<sub>2</sub> + CH<sub>4</sub>. *Fluid Phase Equilib* 2016;413:28–35. <https://doi.org/10.1016/J.FLUID.2015.09.042>.
- [134] Rodriguez CT, Le Q Du, Focsa C, Pirim C, Chazallon B. Influence of crystallization parameters on guest selectivity and structures in a CO<sub>2</sub>-based separation process using TBAB semi-clathrate hydrates. *Chem Eng J* 2020;382:122867. <https://doi.org/10.1016/J.CEJ.2019.122867>.
- [135] Dyadin YA, Udachin KA. Clathrate polyhydrates of peralkylonium salts and their analogs. *J Struct Chem* 1987 283 1987;(28):394–432. <https://doi.org/10.1007/BF00753818>.
- [136] Aminnaji M. Inhibition and dissociation of gas hydrates using glycols/alcohols and biodegradable kinetic hydrate inhibitors. Heriot-Watt University; 2018. Doctoral dissertation.
- [137] Qureshi MF, Attilhan M, Altamash T, Aparicio S, Aminnaji M, Tohidi B. High-pressure gas hydrate autoclave hydraulic experiments and scale-up modeling on the effect of stirring RPM effect. *J Nat Gas Sci Eng* 2017;38:50–8.
- [138] Sun S, Peng X, Zhang Y, Zhao J, Kong Y. Stochastic nature of nucleation and growth kinetics of THF hydrate. *J Chem Thermodyn* 2017;107:141–52.
- [139] Zatsepina OY, Buffett BA. Nucleation of CO<sub>2</sub>-hydrate in a porous medium. *Fluid Phase Equilib* 2002;200:263–75.
- [140] Uchida T, Yamazaki K, Gohara K. Gas nanobubbles as nucleation acceleration in the gas-hydrate memory effect. *J Phys Chem C* 2016;120:26620–9.
- [141] Sabil KM, Duarte ARC, Zevenbergen J, Ahmad MM, Yusup S, Omar AA, et al. Kinetic of formation for single carbon dioxide and mixed carbon dioxide and tetrahydrofuran hydrates in water and sodium chloride aqueous solution. *Int J Greenh Gas Control* 2010;4:798–805.
- [142] Moeini H, Bonyadi M, Esmaelzadeh F, Rasoolzadeh A. Experimental study of sodium chloride aqueous solution effect on the kinetic parameters of carbon dioxide hydrate formation in the presence/absence of magnetic field. *J Nat Gas Sci Eng* 2018;50:231–9.
- [143] Li A, Jiang L, Tang S. An experimental study on carbon dioxide hydrate formation using a gas-inducing agitated reactor. *Energy* 2017;134:629–37.
- [144] Aminnaji M, Anderson R, Hase A, Tohidi B. Can kinetic hydrate inhibitors inhibit the growth of pre-formed gas hydrates? *J Nat Gas Sci Eng* 2022;109:104831.
- [145] He Z, Linga P, Jiang J. What are the key factors governing the nucleation of CO<sub>2</sub> hydrate? *Phys Chem Chem Phys* 2017;19:15657–61.
- [146] Zhang Z, Kusalik PG, Guo G-J. Bridging solution properties to gas hydrate nucleation through guest dynamics. *Phys Chem Chem Phys* 2018;20:24535–8. <https://doi.org/10.1039/C8CP04466J>.
- [147] Mitterdorfer C, Bauer M, Loerting T. Clathrate hydrate formation after CO<sub>2</sub>-H<sub>2</sub>O vapour deposition. *Phys Chem Chem Phys* 2011;13:19765–72. <https://doi.org/10.1039/C1CP21856E>.
- [148] Englezos P, Bishnoi PR. Gibbs free energy analysis for the supersaturation limits of methane in liquid water and the hydrate-gas-liquid water phase behavior. *Fluid Phase Equilib* 1988;42:129–40.
- [149] Englezos P, Kalogerakis N, Dholabhai PD, Bishnoi PR. Kinetics of gas hydrate formation from mixtures of methane and ethane. *Chem Eng Sci* 1987;42:2659–66.
- [150] Christiansen RL, Sloan ED. Mechanisms and kinetics of hydrate formation. *Ann N Y Acad Sci* 1994;715:283–305.
- [151] Kvamme B. A new theory for the kinetics of hydrate formation. *Proc Second Int Conf Nat Gas Hydrates* 1996:131–46. Toulouse, Fr.
- [152] Radhakrishnan R, Trout BL. A new approach for studying nucleation phenomena using molecular simulations: application to CO<sub>2</sub> hydrate clathrates. *J Chem Phys* 2002;117:1786–96.
- [153] Jacobson LC, Hujo W, Molinero V. Amorphous precursors in the nucleation of clathrate hydrates. *J Am Chem Soc* 2010;132:11806–11.
- [154] Vatamanu J, Kusalik PG. Observation of two-step nucleation in methane hydrates. *Phys Chem Chem Phys* 2010;12:15065–72.
- [155] Zhang Z, Walsh MR, Guo G-J. Microcanonical molecular simulations of methane hydrate nucleation and growth: evidence that direct nucleation to sI hydrate is among the multiple nucleation pathways. *Phys Chem Chem Phys* 2015;17: 8870–6.
- [156] Walsh MR, Rainey JD, Lafond PG, Park D-H, Beckham GT, Jones MD, et al. The cages, dynamics, and structuring of incipient methane clathrate hydrates. *Phys Chem Chem Phys* 2011;13:19951–9.
- [157] Bi Y, Li T. Probing methane hydrate nucleation through the forward flux sampling method. *J Phys Chem B* 2014;118:13324–32.
- [158] Natarajan V, Bishnoi PR, Kalogerakis N. Induction phenomena in gas hydrate nucleation. *Chem Eng Sci* 1994;49:2075–87.
- [159] Thoutam P, Rezaei Gomari S, Ahmad F, Islam M. Comparative analysis of hydrate nucleation for methane and carbon dioxide. *Molecules* 2019;24:1055.
- [160] Kvamme B, Graue A, Aspnes E, Kuznetsova T, Gránásy L, Tóth G, et al. Kinetics of solid hydrate formation by carbon dioxide: phase field theory of hydrate nucleation and magnetic resonance imaging. *Phys Chem Chem Phys* 2004;6: 2327–34.
- [161] Tegze G, Pusztai T, Tóth G, Gránásy L, Svandal A, Buanes T, et al. Multiscale approach to CO<sub>2</sub> hydrate formation in aqueous solution: phase field theory and molecular dynamics. *Nucleation and growth. J Chem Phys* 2006;124:234710.
- [162] Liu C, Zhou X, Liang D. Molecular insight into carbon dioxide hydrate formation from saline solution. *RSC Adv* 2021;11:31583–9.
- [163] Mochizuki T, Mori YH. Clathrate-hydrate film growth along water/hydrate-former phase boundaries—numerical heat-transfer study. *J Cryst Growth* 2006; 290:642–52.
- [164] Mori YH. Estimating the thickness of hydrate films from their lateral growth rates: application of a simplified heat transfer model. *J Cryst Growth* 2001;223:206–12.
- [165] Uchida T, Ebinuma T, Kawabata J, Narita H. Microscopic observations of formation processes of clathrate-hydrate films at an interface between water and carbon dioxide. *J Cryst Growth* 1999;204:348–56.
- [166] Peng B, Sun C, Chen G, Yang L, Zhou W, Pang W. Hydrate film growth at the interface between gaseous CO<sub>2</sub> and sodium chloride solution. *Sci China Ser B Chem* 2009;52:676–82.
- [167] Zhou H, Ferreira CI. Effect of type-III Anti-Freeze Proteins (AFPs) on CO<sub>2</sub> hydrate formation rate. *Chem Eng Sci* 2017;167:42–53.
- [168] Clarke MA, Bishnoi PR. Determination of the intrinsic kinetics of CO<sub>2</sub> gas hydrate formation using in situ particle size analysis. *Chem Eng Sci* 2005;60:695–709.
- [169] Malegaonkar MB, Dholabhai PD, Bishnoi PR. Kinetics of carbon dioxide and methane hydrate formation. *Can J Chem Eng* 1997;75:1090–9.
- [170] Chun M-K, Lee H. Kinetics of formation of carbon dioxide clathrate hydrates. *Korean J Chem Eng* 1996;13:620–6.
- [171] Yang D, Le LA, Martinez RJ, Currier RP, Spencer DF. Kinetics of CO<sub>2</sub> hydrate formation in a continuous flow reactor. *Chem Eng J* 2011;172:144–57.
- [172] Fan S, Li S, Wang J, Lang X, Wang Y. Efficient capture of CO<sub>2</sub> from simulated flue gas by formation of TBAB or TBAF semiclathrate hydrates. *Energy & Fuels* 2009; 23:4202–8.
- [173] Uddin M, Coombe D, Law D, Gunter B. Numerical studies of gas hydrate formation and decomposition in a geological reservoir. *J Energy Resour Technol* 2008;130.
- [174] Ota M, Abe Y, Watanabe M, Smith Jr RL, Inomata H. Methane recovery from methane hydrate using pressurized CO<sub>2</sub>. *Fluid Phase Equilib* 2005;228:553–9.
- [175] Sarshar M, Esmaelzadeh F, Fathikalajahi J. Study of capturing emitted CO<sub>2</sub> in the form of hydrates in a tubular reactor. *Chem Eng Commun* 2009;196:1348–65.
- [176] Aya I, Yamane K, Narai H. Solubility of CO<sub>2</sub> and density of CO<sub>2</sub> hydrate at 30 MPa. *Energy* 1997;22:263–71. [https://doi.org/10.1016/S0360-5442\(96\)00093-X](https://doi.org/10.1016/S0360-5442(96)00093-X).
- [177] Bozzo AT, Hsiao-Sheng C, Kass JR, Barduhn AJ. The properties of the hydrates of chlorine and carbon dioxide. *Desalination* 1975;16:303–20. [https://doi.org/10.1016/S0011-9164\(00\)88004-2](https://doi.org/10.1016/S0011-9164(00)88004-2).
- [178] Fournaison L, Delahaye A, Chatti I, Petitet J-P. CO<sub>2</sub> hydrates in refrigeration processes. *Ind Eng Chem Res* 2004;43:6521–6.
- [179] Sabil KM, Wiltcamp GJ, Peters CJ. Estimations of enthalpies of dissociation of simple and mixed carbon dioxide hydrates from phase equilibrium data. *Fluid Phase Equilib* 2010;290:109–14. <https://doi.org/10.1016/J.FLUID.2009.07.006>.
- [180] Lirio CFS, Pessoa FLP. Enthalpy of dissociation of simple and mixed carbon dioxide clathrate hydrate. *Chem Eng Trans* 2013;32:577–82. <https://doi.org/10.3303/CET1332097>.
- [181] Ohgaki K, Makihara Y, Takano K. Formation of CO<sub>2</sub> hydrate in pure and sea waters. *J Chem Eng Japan* 1993;26:558–64.
- [182] Kang SP, Lee H, Ryu BJ. Enthalpies of dissociation of clathrate hydrates of carbon dioxide, nitrogen, (carbon dioxide + nitrogen), and (carbon dioxide + nitrogen + tetrahydrofuran). *J Chem Thermodyn* 2001;33:513–21. <https://doi.org/10.1006/JCHT.2000.0765>.
- [183] Ikeda T, Yamamoto O, Matsuo T, Mori K, Torii S, Kamiyama T, et al. Neutron diffraction study of carbon dioxide clathrate hydrate. *J Phys Chem Solids* 1999; 60:1527–9. [https://doi.org/10.1016/S0022-3697\(99\)00165-1](https://doi.org/10.1016/S0022-3697(99)00165-1).
- [184] Hester KC, Huo Z, Ballard AL, Koh CA, Miller KT, Sloan ED. Thermal expansivity for sI and sII clathrate hydrates. *J Phys Chem B* 2007;111:8830–5. <https://doi.org/10.1021/JP0715880>.
- [185] Hansen TC, Falenty A, Kuhs WF. Lattice constants and expansivities of gas hydrates from 10 K up to the stability limit. *J Chem Phys* 2016;144:054301. <https://doi.org/10.1063/1.4940729>.
- [186] Circone S, Stern LA, Kirby SH, Durham WB, Chakoumakos BC, Rawn CJ, et al. CO<sub>2</sub> hydrate: synthesis, composition, structure, dissociation behavior, and a comparison to structure I CH<sub>4</sub> hydrate. *J Phys Chem B* 2003;107:5529–39. <https://doi.org/10.1021/JP027391J>.
- [187] Beloshudov RV, Zhdanov RK, Bozhko YY, Gets KV, Subbotin OS, Kawazoe Y, et al. Lattice dynamics study of the thermal expansion of C<sub>3</sub>H<sub>8</sub>, CH<sub>4</sub>, CF<sub>4</sub>, CO<sub>2</sub>, Xe-, and N<sub>2</sub>-hydrates. *Energy and Fuels* 2020;34:12771–8. [https://doi.org/10.1021/ACS.ENERGYFUELS.0C01872.SI\\_001.PDF](https://doi.org/10.1021/ACS.ENERGYFUELS.0C01872.SI_001.PDF).
- [188] Ning FL, Glavatskiy K, Ji Z, Kjelstrup S, Vlugt TJ H. Compressibility, thermal expansion coefficient and heat capacity of CH<sub>4</sub> and CO<sub>2</sub> hydrate mixtures using molecular dynamics simulations. *Phys Chem Chem Phys* 2014;17:2869–83. <https://doi.org/10.1039/C4CP04212C>.
- [189] Costandy J, Michalis VK, Tsimplanogiannis IN, Stubos AK, Economou IG. Molecular dynamics simulations of pure methane and carbon dioxide hydrates: lattice constants and derivative properties. *Energy* 2016;114:2672–87. <https://doi.org/10.1080/00268976.2016.1241442>.
- [190] Shicai S, Linlin G, Zhendong Y, Haifei L, Yanmin L. Thermophysical properties of natural gas hydrates: a review. *Nat Gas Ind B* 2022. <https://doi.org/10.1016/J.NGIB.2022.04.003>.
- [191] Mathews SL, Servio PD, Rey AD. Heat capacity, thermal expansion coefficient, and Grüneisen parameter of CH<sub>4</sub>, CO<sub>2</sub>, and C<sub>2</sub>H<sub>6</sub> hydrates and ice Ih via density functional theory and phonon calculations. *Cryst Growth Des* 2020;20:5947–55. [https://doi.org/10.1021/ACS.CGD.0C00630/SUPPL\\_FILE/CG0C00630\\_SI\\_001.PDF](https://doi.org/10.1021/ACS.CGD.0C00630/SUPPL_FILE/CG0C00630_SI_001.PDF).

- [192] Uchida T, Kawabata J. Measurements of mechanical properties of the liquid CO<sub>2</sub>-water-CO<sub>2</sub> hydrate system. *Energy* 1997;22:357–61. [https://doi.org/10.1016/S0360-5442\(96\)00112-0](https://doi.org/10.1016/S0360-5442(96)00112-0).
- [193] Chi Y, Xu Y, Zhao C, Zhang Y, Song Y. In-situ measurement of interfacial tension: further insights into effect of interfacial tension on the kinetics of CO<sub>2</sub> hydrate formation. *Energy* 2022;239:122143. <https://doi.org/10.1016/J.ENERGY.2021.122143>.
- [194] Xia J, Jödecke M, Kamps APS, Maurer G. Solubility of CO<sub>2</sub> in (CH<sub>3</sub>OH + H<sub>2</sub>O). *J Chem Eng Data* 2004;49:1756–9. <https://doi.org/10.1021/JE049803I>.
- [195] Wang LK, Chen GJ, Han GH, Guo XQ, Guo TM. Experimental study on the solubility of natural gas components in water with or without hydrate inhibitor. *Fluid Phase Equilib* 2003;207:143–54. [https://doi.org/10.1016/S0378-3812\(03\)00009-8](https://doi.org/10.1016/S0378-3812(03)00009-8).
- [196] Aminnaji M. Improving the accuracy of experimental hydrate equilibrium point determination: a mini-review. *Petroleum Eng J* 2023;7. <https://doi.org/10.23880/ppej-16000355>.
- [197] Adisasmro S, Frank RJ, Dandy Sloan E. Hydrates of carbon dioxide and methane mixtures. *J Chem Eng, Data* 1991;36:68–71.
- [198] Beltrán JG, Servio P. Equilibrium studies for the system methane + carbon dioxide + neohexane + water. *J Chem Eng Data* 2008;53:1745–9. [https://doi.org/10.1021/JE800066Q/SUPPL\\_FILE/JE800066Q-FILE002.PDF](https://doi.org/10.1021/JE800066Q/SUPPL_FILE/JE800066Q-FILE002.PDF).
- [199] Sadeq D, Iglauser S, Lebedev M, Smith C, Barifcanci A. Experimental determination of hydrate phase equilibrium for different gas mixtures containing methane, carbon dioxide and nitrogen with motor current measurements. *J Nat Gas Sci Eng* 2017;38:59–73.
- [200] Lafond PG, Olcott KA, Dendy Sloan E, Koh CA, Sum AK. Measurements of methane hydrate equilibrium in systems inhibited with NaCl and methanol. *J Chem Thermodyn* 2012;48:1–6. <https://doi.org/10.1016/J.JCT.2011.12.023>.
- [201] Wells JD, Chen W, Hartman RL, Koh CA. Carbon dioxide hydrate in a microfluidic device: phase boundary and crystallization kinetics measurements with micro-Raman spectroscopy. *J Chem Phys* 2021;154:114710. <https://doi.org/10.1063/5.0039533>.
- [202] Tohidi B, Burgass RW, Danesh A, Østergaard KK, Todd AC. Improving the accuracy of gas hydrate dissociation point measurements. *Ann N Y Acad Sci* 2000; 912:924–31.
- [203] Sayani JKS, Lal B, Pedapati SR. Comprehensive review on various gas hydrate modelling techniques: prospects and challenges. *Arch Comput Methods Eng* 2021; 1–37.
- [204] Mahabadian MA, Chapoy A, Burgass R, Tohidi B. Development of a multiphase flash in presence of hydrates: experimental measurements and validation with the CPA equation of state. *Fluid Phase Equilib* 2016;414:117–32. <https://doi.org/10.1016/J.FLUID.2016.01.009>.
- [205] Zhang X, Pedrosa N, Szczepanski R. Modelling salts effect on hydrate inhibition with CPA-electrolyte and pseudo-salt approach with excess Gibbs energy mixing rules. *Upstream eng. Flow assur. AICHH 2017 spring meet. San antonio (conference pap. Kindly provid. Dr. Zhang); 2017*.
- [206] Zhang G, Li J, Liu G, Yang H, Huang H. Applicability research of thermodynamic models of gas hydrate phase equilibrium based on different equations of state. *RSC Adv* 2022;12:15870–84. <https://doi.org/10.1039/D2RA00875K>.
- [207] Vidal-Vidal Á, Pérez-Rodríguez M, Torré J-P, Piñeiro MM. DFT calculation of the potential energy landscape topology and Raman spectra of type I CH<sub>4</sub> and CO<sub>2</sub> hydrates. *Phys Chem Chem Phys* 2015;17:6963–75. <https://doi.org/10.1039/C4CP04962D>.
- [208] Ma Z, Ranjith PG. Review of application of molecular dynamics simulations in geological sequestration of carbon dioxide. *Fuel* 2019;255:115644. <https://doi.org/10.1016/J.FUEL.2019.115644>.
- [209] Yi L, Liang D, Zhou X, Li D. Molecular dynamics simulations for the growth of CH<sub>4</sub>-CO<sub>2</sub> mixed hydrate. *J Energy Chem* 2014;23:747–54. [https://doi.org/10.1016/S2095-4956\(14\)60208-4](https://doi.org/10.1016/S2095-4956(14)60208-4).
- [210] Liu N, Zhou J, Hong C. Molecular dynamics simulations on dissociation of CO<sub>2</sub> hydrate in the presence of inhibitor. *Chem Phys* 2020;538:110894. <https://doi.org/10.1016/J.CHEMPHYS.2020.110894>.
- [211] Qi Y, Ota M, Zhang H. Molecular dynamics simulation of replacement of CH<sub>4</sub> in hydrate with CO<sub>2</sub>. *Energy Convers Manag* 2011;52:2682–7. <https://doi.org/10.1016/J.ENCONMAN.2011.01.020>.
- [212] Zhang L, Sun L, Lu Y, Kuang Y, Ling Z, Yang L, et al. Molecular dynamics simulation and in-situ MRI observation of organic exclusion during CO<sub>2</sub> hydrate growth. *Chem Phys Lett* 2021;764:138287. <https://doi.org/10.1016/J.CPLETT.2020.138287>.
- [213] Míguez JM, Conde MM, Torré JP, Blas FJ, Piñeiro MM, Vega C. Molecular dynamics simulation of CO<sub>2</sub> hydrates: prediction of three phase coexistence line. *J Chem Phys* 2015;142:124505. <https://doi.org/10.1063/1.4916119>.
- [214] Jiao L, Wang Z, Li J, Zhao P, Wan R. Stability and dissociation studies of CO<sub>2</sub> hydrate under different systems using molecular dynamic simulations. *J Mol Liq* 2021;338:116788. <https://doi.org/10.1016/J.MOLLIQ.2021.116788>.
- [215] Tung YT, Chen LJ, Chen YP, Lin ST. Growth of structure I carbon dioxide hydrate from molecular dynamics simulations. *J Phys Chem C* 2011;115:7504–15. <https://doi.org/10.1021/JP112205X>.
- [216] Wendland M, Hasse H, Maurer G. Experimental Pressure–Temperature data on three- and four-phase equilibria of fluid, hydrate, and ice phases in the system carbon Dioxide–Water. *J Chem Eng Data* 1999;44:901–6. <https://doi.org/10.1021/JE9802080>.
- [217] Ye N, Zhang P. Equilibrium data and morphology of tetra-n-butyl ammonium bromide semiclathrate hydrate with carbon dioxide. *J Chem Eng Data* 2012;57: 1557–62. [https://doi.org/10.1021/JE3001443/ASSET/IMAGES/MEDIUM/JE-2012-001443\\_0008](https://doi.org/10.1021/JE3001443/ASSET/IMAGES/MEDIUM/JE-2012-001443_0008).
- [218] Takenouchi S, Kennedy GC. Dissociation pressures of the phase CO<sub>2</sub>-5 3/4 H<sub>2</sub>O. *J Geol* 1965;73:383–90.
- [219] Ng HJ, Robinson DB. Hydrate formation in systems containing methane, ethane, propane, carbon dioxide or hydrogen sulfide in the presence of methanol. *Fluid Phase Equilib* 1985;21:145–55. [https://doi.org/10.1016/0378-3812\(85\)90065-2](https://doi.org/10.1016/0378-3812(85)90065-2).
- [220] Seo YT, Lee H, Yoon JH. Hydrate phase equilibria of the carbon dioxide, methane, and water system. *J Chem Eng Data* 2001;46:381–4. <https://doi.org/10.1021/JE000237A>.
- [221] Mel'nikov VP, Nesterov AN, Podenko LS, Reshetnikov AM. Influence of carbon dioxide on melting of underground ice. *Dokl Earth Sci* 2014;459:1353.
- [222] Nakano S, Moritoki M, Ohgaki K. High-pressure phase equilibrium and Raman microprobe spectroscopic studies on the CO<sub>2</sub> hydrate system. *J Chem \& Eng Data* 1998;43:807–10.
- [223] Bollengier O, Choukroun M, Grasset O, Le Menn EL, Bellino G, Morizet Y, et al. Phase equilibria in the H<sub>2</sub>O–CO<sub>2</sub> system between 250–330 K and 0–1.7 GPa: stability of the CO<sub>2</sub> hydrates and H<sub>2</sub>O-ice VI at CO<sub>2</sub> saturation. *Geochim Cosmochim Acta* 2013;119:322–39. <https://doi.org/10.1016/J.GCA.2013.06.006>.
- [224] Manakov AY, Dyadin YA, Ogienko AG, Kurnosov AV, Aladko EY, Larionov EG, et al. Phase diagram and high-pressure boundary of hydrate formation in the carbon dioxide–water system. *J Phys Chem B* 2009;113:7257–62.
- [225] Dorman P, Alavi S, Woo TK. Free energies of carbon dioxide sequestration and methane recovery in clathrate hydrates. *J Chem Phys* 2007;127:124510.
- [226] Gambelli AM, Presciutti A, Rossi F. Review on the characteristics and advantages related to the use of flue-gas as CO<sub>2</sub>/N<sub>2</sub> mixture for gas hydrate production. *Fluid Phase Equilib* 2021;541:113077.
- [227] Hassanpourouzband A, Yang J, Tohidi B, Chuivilin E, Istomin V, Bukhanov B, et al. CO<sub>2</sub> capture by injection of flue gas or CO<sub>2</sub>-N<sub>2</sub> mixtures into hydrate reservoirs: dependence of CO<sub>2</sub> capture efficiency on gas hydrate reservoir conditions. *Environ Sci \& Technol* 2018;52:4324–30.
- [228] Hassanpourouzband A, Yang J, Okwananek A, Burgass R, Tohidi B, Chuivilin E, et al. An experimental investigation on the kinetics of integrated methane recovery and CO<sub>2</sub> sequestration by injection of flue gas into permafrost methane hydrate reservoirs. *Sci Rep* 2019;9:1–9.
- [229] Sun S-C, Liu C-L, Meng Q-G. Hydrate phase equilibrium of binary guest-mixtures containing CO<sub>2</sub> and N<sub>2</sub> in various systems. *J Chem Thermodyn* 2015;84:1–6.
- [230] Jarrahan A, Nakhaei A. Hydrate–liquid–vapor equilibrium condition of N<sub>2</sub>+CO<sub>2</sub>+H<sub>2</sub>O system: measurement and modeling. *Fuel* 2019;237:769–74.
- [231] Zang X, Wan L, Liang D. Investigation of the hydrate formation process in fine sediments by a binary CO<sub>2</sub>/N<sub>2</sub> gas mixture. *Chinese J Chem Eng* 2019;27: 2157–63.
- [232] Hosseini G, Mohebbi V. Thermodynamic modeling of gas hydrate phase equilibrium of carbon dioxide and its mixture using different equations of states. *J Chem Thermodyn* 2022;106834.
- [233] Nohra M, Woo TK, Alavi S, Ripmeester JA. Molecular dynamics Gibbs free energy calculations for CO<sub>2</sub> capture and storage in structure I clathrate hydrates in the presence of SO<sub>2</sub>, CH<sub>4</sub>, N<sub>2</sub>, and H<sub>2</sub>S impurities. *J Chem Thermodyn* 2012;44: 5–12.
- [234] Kvamme B, Iden E, Tveit J, Veland V, Zarifi M, Qorbani K. Effect of H<sub>2</sub>S content on thermodynamic stability of hydrate formed from CO<sub>2</sub>/N<sub>2</sub> mixtures. *J Chem Eng Data* 2017;62:1645–58.
- [235] Daraboina N, Ripmeester J, Englezos P. The impact of SO<sub>2</sub> on post combustion carbon dioxide capture in bed of silica sand through hydrate formation. *Int J Greenh Gas Control* 2013;15:97–103.
- [236] Ward ZT, Deering CE, Marriott RA, Sum AK, Sloan ED, Koh CA. Phase equilibrium data and model comparisons for H<sub>2</sub>S hydrates. *J Chem \& Eng Data* 2015;60: 403–8.
- [237] Beeskow-Strauch B, Schicks JM, Spangenberg E, Erzinger J. The influence of SO<sub>2</sub> and NO<sub>2</sub> impurities on CO<sub>2</sub> gas hydrate formation and stability. *Chem Eur J* 2011;17:4376–84.
- [238] Chapoy A, Burgass R, Tohidi B, Alsiyabi I. Hydrate and phase behavior modeling in CO<sub>2</sub>-rich pipelines. *J Chem \& Eng Data* 2015;60:447–53.
- [239] Herri J-M, Bouchemoua A, Kwaterski M, Fezoua A, Ouabbas Y, Cameirão A. Gas hydrate equilibria for CO<sub>2</sub>-N<sub>2</sub> and CO<sub>2</sub>-CH<sub>4</sub> gas mixtures—experimental studies and thermodynamic modelling. *Fluid Phase Equilib* 2011;301:171–90.
- [240] Zheng R, Fan Z, Li X, Negahban S. Phase boundary of CH<sub>4</sub>, CO<sub>2</sub>, and binary CH<sub>4</sub>-CO<sub>2</sub> hydrates formed in NaCl solutions. *J Chem Thermodyn* 2021;154:106333.
- [241] Zheng R, Li X, Negahban S. Phase boundary of gas hydrates in single and mixed electrolyte solutions: using a novel unified equation of state. *J Mol Liq* 2022;345: 117825. <https://doi.org/10.1016/J.MOLLIQ.2021.117825>.
- [242] Legoux LN, Ruffine L, Deusner C, Haeckel M. Experimental study of mixed gas hydrates from gas feed containing CH<sub>4</sub>, CO<sub>2</sub> and N<sub>2</sub>: phase equilibrium in the presence of excess water and gas exchange. *Energies* 2018;11:1984.
- [243] Zang X, Wang J, Zhou X, Wan L, Liang D. Phase equilibria of the synthesized ternary CH<sub>4</sub>/CO<sub>2</sub>/N<sub>2</sub> mixed-gas hydrates in tetrabutylammonium bromide aqueous solutions at different concentrations. *J Chem Eng Data* 2021;66:1290–5.
- [244] Li L, Fan S, Chen Q, Yang G, Zhao J, Wei N, et al. Experimental and modeling phase equilibria of gas hydrate systems for post-combustion CO<sub>2</sub> capture. *J Taiwan Inst Chem Eng* 2019;96:35–44.
- [245] Chazallon B, Pirim C. Selectivity and CO<sub>2</sub> capture efficiency in CO<sub>2</sub>-N<sub>2</sub> clathrate hydrates investigated by in-situ Raman spectroscopy. *Chem Eng J* 2018;342: 171–83. <https://doi.org/10.1016/J.CEJ.2018.01.116>.
- [246] Kuhs WF, Chazallon B, Radaelli PG, Pauer F. Cage occupancy and compressibility of deuterated N<sub>2</sub>-clathrate hydrate by neutron diffraction. *J Incl Phenom Mol Recognit Chem* 1997;29:65–77.

- [247] Manakov AY, Voronin VI, Kurnosov AV, Teplykh AE, Komarov VY, Dyadin YA. Structural investigations of argon hydrates at pressures up to 10 kbar. *J Incl Phenom Macrocycl Chem* 2004;48:11–8.
- [248] Tse JS, Handa YP, Ratcliffe CI, Powell BM. Structure of oxygen clathrate hydrate by neutron powder diffraction. *J Incl Phenom* 1986;43:1986;(4):235–40. <https://doi.org/10.1007/BF00657996>.
- [249] Schicks JM, Luzi M, Spangenberg E, Naumann R, Erzinger J. Hydrate formation investigations and kinetic studies under various defined conditions. 2008.
- [250] Schicks JM. Gas hydrates: formation, structures, and properties. *Hydrocarb oils lipids divers orig chem fate*. 2020. p. 81–95.
- [251] Babakhani SM, Ho-Van S, Bouillot B, Douzet J, Herri J-M. Phase equilibrium measurements and modelling of mixed cyclopentane and carbon dioxide hydrates in presence of salts. *Chem Eng Sci* 2020;214:115442.
- [252] Sun Y-F, Zhong J-R, Li R, Zhu T, Cao X-Y, Chen G-J, et al. Natural gas hydrate exploitation by CO<sub>2</sub>/H<sub>2</sub> continuous Injection-Production mode. *Appl Energy* 2018;226:10–21.
- [253] Chaturvedi KR, Sinha ASK, Nair VC, Sharma T. Enhanced carbon dioxide sequestration by direct injection of flue gas doped with hydrogen into hydrate reservoir: possibility of natural gas production. *Energy* 2021;227:120521.
- [254] Sun Y-F, Wang Y-F, Zhong J-R, Li W-Z, Li R, Cao B-J, et al. Gas hydrate exploitation using CO<sub>2</sub>/H<sub>2</sub> mixture gas by semi-continuous injection-production mode. *Appl Energy* 2019;240:215–25.
- [255] Veluswamy HP, Kumar R, Linga P. Hydrogen storage in clathrate hydrates: current state of the art and future directions. *Appl Energy* 2014;122:112–32.
- [256] Xu C-G, Zhang S-H, Cai J, Chen Z-Y, Li X-S. CO<sub>2</sub> (carbon dioxide) separation from CO<sub>2</sub>-H<sub>2</sub> (hydrogen) gas mixtures by gas hydrates in TBAB (tetra-n-butyl ammonium bromide) solution and Raman spectroscopic analysis. *Energy* 2013;59:719–25.
- [257] Xie Y, Zheng T, Zhu Y-J, Zhong J-R, Feng J-C, Sun C-Y, et al. Effects of H<sub>2</sub>/N<sub>2</sub> on CO<sub>2</sub> hydrate film growth: morphology and microstructure. *Chem Eng J* 2022;431:134004.
- [258] Mao WL, Mao H, Goncharov AF, Struzhkin NV, Guo Q, Hu J, et al. Hydrogen clusters in clathrate hydrate. *Science* 2002;297:2247–9.
- [259] Xie Y, Zhu Y-J, Cheng L-W, Zheng T, Zhong J-R, Xiao P, et al. The coexistence of multiple hydrates triggered by varied H<sub>2</sub> molecule occupancy during CO<sub>2</sub>/H<sub>2</sub> hydrate dissociation. *Energy* 2022;125461.
- [260] Kumar R, Englezos P, Moudrakovsky I, Ripmeester JA. Structure and composition of CO<sub>2</sub>/H<sub>2</sub> and CO<sub>2</sub>/H<sub>2</sub>/C3H<sub>8</sub> hydrate in relation to simultaneous CO<sub>2</sub> capture and H<sub>2</sub> production. *AICHE J* 2009;55:1584–94.
- [261] Lu H, Wang J, Liu C, Ratcliffe CI, Becker U, Kumar R, et al. Multiple H<sub>2</sub> occupancy of cages of clathrate hydrate under mild conditions. *J Am Chem Soc* 2012;134:9160–2.
- [262] Skiba S, Chashchin D, Semenov A, Yarakhmedov M, Vinokurov V, Sagidullin A, et al. Hydrate-based separation of the CO<sub>2</sub>+ H<sub>2</sub> mixtures. Phase equilibria with isopropanol aqueous solutions and hydrogen solubility in CO<sub>2</sub> hydrate. *Int J Hydrogen Energy* 2021;46:32904–13.
- [263] Burnol A, Thinon I, Ruffine L, Herri J-M. Influence of impurities (nitrogen and methane) on the CO<sub>2</sub> storage capacity as sediment-hosted gas hydrates—Application in the area of the Celtic Sea and the Bay of Biscay. *Int J Greenh Gas Control* 2015;35:96–109.
- [264] Bruusgaard H, Beltrán JG, Servio P. Solubility measurements for the CH<sub>4</sub>+ CO<sub>2</sub>+ H<sub>2</sub>O system under hydrate–liquid–vapor equilibrium. *Fluid Phase Equilib* 2010;296:106–9.
- [265] Bruusgaard H, Servio P. Prediction of methane and carbon dioxide solubilities for the CH<sub>4</sub>+ CO<sub>2</sub>+ H<sub>2</sub>O system under hydrate–liquid–vapor equilibrium. *Fluid Phase Equilib* 2011;305:97–100.
- [266] Lang F, Servio P. Solubility measurements for the N<sub>2</sub>+ CO<sub>2</sub>+ H<sub>2</sub>O system under hydrate–liquid–vapor equilibrium. *J Chem Eng Data* 2014;59:2547–50.
- [267] Lang F, Servio P. Solubility measurements for the CH<sub>4</sub>+ C<sub>2</sub>H<sub>6</sub>+ H<sub>2</sub>O system under hydrate–liquid–vapour equilibrium. *J Nat Gas Sci Eng* 2015;26:130–4.
- [268] Chapoy A, Nazeri M, Kapatéh M, Burgass R, Coquelet C, Tohidi B. Effect of impurities on thermophysical properties and phase behaviour of a CO<sub>2</sub>-rich system in CCS. *Int J Greenh Gas Control* 2013;19:92–100. <https://doi.org/10.1016/J.IJGGC.2013.08.019>.
- [269] Liu N, Zhu H, Zhou J, Yang L, Liu D. Molecular dynamics simulations on formation of CO<sub>2</sub> hydrate in the presence of metal particles. *J Mol Liq* 2021;331:115793. <https://doi.org/10.1016/J.MOLLIQ.2021.115793>.
- [270] Bozorgian AR, Arab Aboosadi Z, Mohammadi A, Honavar B, Azimi AR. Statistical analysis of the effects of aluminum oxide (Al<sub>2</sub>O<sub>3</sub>) nanoparticle, TBAC, and APG on storage capacity of CO<sub>2</sub> hydrate formation. *Iran J Chem Chem Eng Res Artic* 2022;41.
- [271] Wang Y, Niu A, Jiao W, Chen J, Zhang P, Li J. Effects of the presence of promoters sodium dodecyl sulfate, nanographite, and tetra-n-butylammonium bromide on the formation of CO<sub>2</sub> hydrates. *Energy & Fuels* 2022;36(17):10269–77.
- [272] Li Y, Gambelli AM, Rossi F, Mei S. Effect of promoters on CO<sub>2</sub> hydrate formation: thermodynamic assessment and microscale Raman spectroscopy/hydrate crystal morphology characterization analysis. *Fluid Phase Equilib* 2021;550:113218.
- [273] Figueira JD, Fout T, Plasynski S, McIlvried H, Srivastava RD. Advances in CO<sub>2</sub> capture technology—the US department of energy's carbon sequestration program. *Int J Greenh Gas Control* 2008;2:9–20.
- [274] Madejski Paweland Chmiel K, Subramanian N, Kuś T. Methods and techniques for CO<sub>2</sub> capture: review of potential solutions and applications in modern energy technologies. *Energies* 2022;15:887.
- [275] Rubin ES, Chen C, Rao AB. Cost and performance of fossil fuel power plants with CO<sub>2</sub> capture and storage. *Energy Policy* 2007;35:4444–54.
- [276] Nord LO, Bolland O. Carbon dioxide emission management in power generation. John Wiley \& Sons; 2020.
- [277] Wang M, Lawal A, Stephenson P, Sidders J, Ramshaw C. Post-combustion CO<sub>2</sub> capture with chemical absorption: a state-of-the-art review. *Chem Eng Res Des* 2011;89:1609–24.
- [278] Wang Y, Zhao L, Otto A, Robinius M, Stoltzen D. A review of post-combustion CO<sub>2</sub> capture technologies from coal-fired power plants. *Energy Procedia* 2017;114:650–65.
- [279] Dashti H, Yew LZ, Lou X. Recent advances in gas hydrate-based CO<sub>2</sub> capture. *J Nat Gas Sci Eng* 2015;23:195–207.
- [280] Matizakurima F, Babaee S, Hashemi H, Naidoo P. Separation of Xenon from Noble gas mixtures of Argon, Krypton, and Xenon using gas hydrate technology. *Industrial & Engineering Chemistry Research* 2023;62(36):14484–96.
- [281] Eslamimanesh A, Mohammadi AH, Richon D, Naidoo P, Ramjugernath D. Application of gas hydrate formation in separation processes: a review of experimental studies. *J Chem Thermodyn* 2012;46:62–71.
- [282] Koh CA, Westacott RE, Zhang W, Hirachand K, Creek JL, Soper AK. Mechanisms of gas hydrate formation and inhibition. *Fluid Phase Equilib* 2002;194:143–51.
- [283] Petuya C, Damay F, Desplanche S, Talaga D, Desmedt A. Selective trapping of CO<sub>2</sub> gas and cage occupancy in CO<sub>2</sub>-N<sub>2</sub> and CO<sub>2</sub>-CO mixed gas hydrates. *Chem Commun* 2018;54:4290–3.
- [284] Currier R, Deppe G, Lee A, Tam SS, Spencer DF. CO<sub>2</sub> capture by formation of hydrates: economical analysis and new promoter process. Alexandria, Virginia: Fifth Annu. Conf. carbon capture \& sequestration; 2006.
- [285] Xu C-G, Li X-S. Research progress of hydrate-based CO<sub>2</sub> separation and capture from gas mixtures. *Rsc Adv* 2014;4:18301–16.
- [286] Yang M, Song Y, Jiang L, Zhu N, Liu Y, Zhao Y, et al. CO<sub>2</sub> hydrate formation and dissociation in cooled porous media: a potential technology for CO<sub>2</sub> capture and storage. *Environ Sci \& Technol* 2013;47:9739–46.
- [287] Dashti H, Underschultz J, Garnett A, Honari V, Sedaghat M, Rudolph V. A review of recent advances in cost-effective infrastructure system design of the CO<sub>2</sub> distribution to CCS injection wells. *SPE asia pacific oil gas conf. Exhib.*; 2018.
- [288] Obara S, Tanaka R. Waste heat recovery system for nuclear power plants using the gas hydrate heat cycle. *Appl Energy* 2021;292:116667.
- [289] Uemura Y, Kawasaki T, Obara S. Analysis of the performance of an electricity generation system using the CO<sub>2</sub> hydrate formation and dissociation process for heat recover. *Energy* 2021;218:119412.
- [290] Wang Y, Lang X, Fan S. Hydrate capture CO<sub>2</sub> from shifted synthesis gas, flue gas and sour natural gas or biogas. *J Energy Chem* 2013;22:39–47.
- [291] Liu G, Zhu L, Cao W, Liu H, He Y. New technique integrating hydrate-based gas separation and chemical absorption for the sweetening of natural gas with high H<sub>2</sub>S and CO<sub>2</sub> contents. *ACS Omega* 2021;6:26180–90.
- [292] Yang M, Zhou H, Wang P, Song Y. Effects of additives on continuous hydrate-based flue gas separation. *Appl Energy* 2018;221:374–85.
- [293] Cheng Z, Li S, Liu Y, Zhang Y, Ling Z, Yang M, et al. Post-combustion CO<sub>2</sub> capture and separation in flue gas based on hydrate technology: a review. *Renew Sustain Energy Rev* 2022;154:111806.
- [294] Delahaye A, Fournaison L, Marinhais S, Chatti I, Petitet J-P, Dalmazzone D, et al. Effect of THF on equilibrium pressure and dissociation enthalpy of CO<sub>2</sub> hydrates applied to secondary refrigeration. *Ind \& Eng Chem Res* 2006;45:391–7.
- [295] Li Z-Y, Xia Z-M, Chen Z-Y, Li X-S, Xu C-G, Yan R. The plateau effects and crystal transition study in tetrahydrofuran (THF)/CO<sub>2</sub>/H<sub>2</sub> hydrate formation processes. *Appl Energy* 2019;238:195–201.
- [296] Zhang Y, Zhao L, Deng S, Zhao R, Nie X, Liu Y. Effect of nanobubble evolution on hydrate process: a review. *J Therm Sci* 2019;28:948–61.
- [297] Nguyen NN, Nguyen AV, Steel KM, Dang LX, Galib M. Interfacial gas enrichment at hydrophobic surfaces and the origin of promotion of gas hydrate formation by hydrophobic solid particles. *J Phys Chem C* 2017;121:3830–40.
- [298] McElligott A, Uddin H, Meunier J-L, Servio P. Effects of hydrophobic and hydrophilic graphene nanoflakes on methane hydrate kinetics. *Energy \& Fuels* 2019;33:11705–11.
- [299] He Z, Mi F, Ning F. Molecular insights into CO<sub>2</sub> hydrate formation in the presence of hydrophilic and hydrophobic solid surfaces. *Energy* 2021;234:121260.
- [300] Liu Y, Zhang L, Yang L, Dong H, Zhao J, Song Y. Behaviors of CO<sub>2</sub> hydrate formation in the presence of acid-dissolvable organic matters. *Environ Sci \& Technol* 2021;55:6206–13.
- [301] Wang P, Teng Y, Zhu J, Bao W, Han S, Li Y, et al. Review on the synergistic effect between metal–organic frameworks and gas hydrates for CH<sub>4</sub> storage and CO<sub>2</sub> separation applications. *Renew Sustain Energy Rev* 2022;167:112807.
- [302] Yan S, Dai W, Wang S, Rao Y, Zhou S. Graphene oxide: an effective promoter for CO<sub>2</sub> hydrate formation. *Energy* 2018;11:1756.
- [303] Liu X, Feng P, Cai Y, Yu X, Yu C, Ran Q. Carbonation behavior of calcium silicate hydrate (CSH): its potential for CO<sub>2</sub> capture. *Chem Eng J* 2022;431:134243.
- [304] Mok J, Choi W, Kim S, Lee J, Seo Y. NaCl-induced enhancement of thermodynamic and kinetic CO<sub>2</sub> selectivity in CO<sub>2</sub>+ N<sub>2</sub> hydrate formation and its significance for CO<sub>2</sub> sequestration. *Chem Eng J* 2023;451:138633.
- [305] Wang H, Lu Y, Zhang X, Fan Q, Li Q, Zhang L, et al. Molecular dynamics of carbon sequestration via forming CO<sub>2</sub> hydrate in a marine environment. *Energy \& Fuels* 2023;37:9309–17.
- [306] Martinez I, Martini M, Riva L, Gallucci F, Annaland MVS, Romano MC. Techno-economic analysis of a natural gas combined cycle integrated with a Ca-Cu looping process for low CO<sub>2</sub> emission power production. *Int J Greenh Gas Control* 2019;81:216–39.
- [307] Rehman A ur, Lal B. Gas hydrate-based CO<sub>2</sub> capture: a journey from batch to continuous. *Energies* 2022;15:8309.

- [308] Phan A, Striolo A. Chemical promoter performance for CO<sub>2</sub> hydrate growth: a molecular perspective. *Energy & Fuels* 2023;37:6002–11.
- [309] He Y, Sun M-T, Chen C, Zhang G-D, Chao K, Lin Y, et al. Surfactant-based promotion to gas hydrate formation for energy storage. *J Mater Chem A* 2019;7: 21634–61.
- [310] Mori YH. On the scale-up of gas-hydrate-forming reactors: the case of gas-dispersion-type reactors. *Energies* 2015;8:1317–35.
- [311] Nguyen NN, La VT, Huynh CD, Nguyen AV. Technical and economic perspectives of hydrate-based carbon dioxide capture. *Appl Energy* 2022;307:118237.
- [312] Rezaei N, Mohebbi V, Feyzi V. Hybrid hydrate processes for CO<sub>2</sub>/H<sub>2</sub> mixture purification: a techno-economic analysis. *Int J Hydrogen Energy* 2022;47: 10137–55.
- [313] Cuellar-Franca RM, Azapagic A. Carbon capture, storage and utilisation technologies: a critical analysis and comparison of their life cycle environmental impacts. *J CO<sub>2</sub> Util* 2015;9:82–102.
- [314] Lv X, Lu D, Liu Y, Zhou S, Zuo J, Jin H, et al. Study on methane hydrate formation in gas-water systems with a new compound promoter. *RSC Adv* 2019;9: 33506–18.
- [315] Esfahimanesh A, Gharagheizi F, Illebeigi M, Mohammadi AH, Fazlali A, Richon D. Phase equilibrium modeling of clathrate hydrates of methane, carbon dioxide, nitrogen, and hydrogen+ water soluble organic promoters using Support Vector Machine algorithm. *Fluid Phase Equilib* 2012;316:34–45.
- [316] Lim J, Choi W, Mok J, Seo Y. Kinetic CO<sub>2</sub> selectivity in clathrate-based CO<sub>2</sub> capture for upgrading CO<sub>2</sub>-rich natural gas and biogas. *Chem Eng J* 2019;369: 686–93.
- [317] Fan S, Li Q, Nie J, Lang X, Wen Y, Wang Y. Semiclathrate hydrate phase equilibrium for CO<sub>2</sub>/CH<sub>4</sub> gas mixtures in the presence of tetrabutylammonium halide (bromide, chloride, or fluoride). *J Chem & Eng Data* 2013;58:3137–41.
- [318] Zheng J, Zhang B-Y, Wu Q, Linga P. Kinetic evaluation of cyclopentane as a promoter for CO<sub>2</sub> capture via a clathrate process employing different contact modes. *ACS Sustain Chem & Eng* 2018;6:11913–21.
- [319] Muromachi S, Udagiri KA, Shin K, Alavi S, Moudrakovski IL, Ohmura R, et al. Guest-induced symmetry lowering of an ionic clathrate material for carbon capture. *Chem Commun* 2014;50:11476–9.
- [320] Ricaurte M, Dicharry C, Renaud X, Torré J-P. Combination of surfactants and organic compounds for boosting CO<sub>2</sub> separation from natural gas by clathrate hydrate formation. *Fuel* 2014;122:206–17.
- [321] Pahlavanzadeh H, Khanlarkhani M, Rezaei S, Mohammadi AH. Experimental and modelling studies on the effects of nanofluids (SiO<sub>2</sub>, Al<sub>2</sub>O<sub>3</sub>, and CuO) and surfactants (SDS and CTAB) on CH<sub>4</sub> and CO<sub>2</sub> clathrate hydrates formation. *Fuel* 2019;253:1392–405.
- [322] Bhattacharjee G, Goh MN, Arumuganainar SEK, Zhang Y, Linga P. Ultra-rapid uptake and the highly stable storage of methane as combustible ice. *Energy & Environ Sci* 2020;13:4946–61.
- [323] Zhang Y, Zhao J, Bhattacharjee G, Xu H, Yang M, Kumar R, et al. Synthesis of methane hydrate at ambient temperature with ultra-rapid formation and high gas storage capacity. *Energy & Environ Sci* 2022;15:5362–78.
- [324] Wang P-W, Wu DT, Lin S-T. Promotion mechanism for the growth of CO<sub>2</sub> hydrate with urea using molecular dynamics simulations. *Chem Commun* 2021;57: 5330–3.
- [325] Wang W, Ma C, Lin P, Sun L, Cooper AI. Gas storage in renewable bioclathrates. *Energy & Environ Sci* 2013;6:105–7.
- [326] Wang Z, Ma G, Shang L, Zhang L. Effect of a nonionic surfactant on the formation of natural gas hydrate in a diesel emulsion system. *Pet Sci Technol* 2018;36: 2017–23.
- [327] Schwenk M, Katzir A, Mizraikoff B. In situ monitoring of additives during CO<sub>2</sub> gas hydrate formation. *Anal Methods* 2016;8:5897–905.
- [328] Liu N, Huang J, Meng F, Yang L. Experimental study on the mechanism of enhanced CO<sub>2</sub> hydrate generation by thermodynamic promoters. *ACS Sustain Chem & Eng* 2023;11:5367–75.
- [329] Hassan MHA, Sher F, Zarren G, Suleiman N, Tahir AA, Snape CE. Kinetic and thermodynamic evaluation of effective combined promoters for CO<sub>2</sub> hydrate formation. *J Nat Gas Sci Eng* 2020;78:103313.
- [330] Zhang F, Wang X, Lou X, Lipiński W. The effect of sodium dodecyl sulfate and dodecyltrimethylammonium chloride on the kinetics of CO<sub>2</sub> hydrate formation in the presence of tetra-n-butyl ammonium bromide for carbon capture applications. *Energy* 2021;227:120424.
- [331] Xu C-G, Yu Y-S, Ding Y-L, Cai J, Li X-S. The effect of hydrate promoters on gas uptake. *Phys Chem Chem Phys* 2017;19:21769–76.
- [332] Burla SK, Pinnelli SRP. Enrichment of gas storage in clathrate hydrates by optimizing the molar liquid water–gas ratio. *RSC Adv* 2022;12:2074–82.
- [333] Veluswamy HP, Kumar A, Kumar R, Linga P. An innovative approach to enhance methane hydrate formation kinetics with leucine for energy storage application. *Appl Energy* 2017;188:190–9.
- [334] Dufour T, Hoang HM, Oignet J, Osswald V, Clain P, Fournaison L, et al. Impact of pressure on the dynamic behavior of CO<sub>2</sub> hydrate slurry in a stirred tank reactor applied to cold thermal energy storage. *Appl Energy* 2017;204:641–52.
- [335] Rossi F, Filippini M, Castellani B. Investigation on a novel reactor for gas hydrate production. *Appl Energy* 2012;99:167–72.
- [336] Szymcek P, McCallum SD, Taboada-Serrano P, Tsouris C. A pilot-scale continuous-jet hydrate reactor. *Chem Eng J* 2008;135:71–7.
- [337] Xu C-G, Yu Y-S, Xie W-J, Xia Z-M, Chen Z-Y, Li X-S. Study on developing a novel continuous separation device and carbon dioxide separation by process of hydrate combined with chemical absorption. *Appl Energy* 2019;255:113791.
- [338] Xue Q, Liu F, Li Z, Wang X, Sun X, Liu M, Wang P, Fan S, Lang X. Hydrate-Based Multistage Biogas Separation Using a Novel Jet Impingement Stream Reactor. *Energy & Fuels* 2023;37(15):11142–51.
- [339] Dashti H, Lou X. Gas hydrate-based CO<sub>2</sub> separation process: quantitative assessment of the effectiveness of various chemical additives involved in the process. *Energy Technol* 2018 Carbon Dioxide Manag Other Technol 2018;3:16.
- [340] Surovtseva D, Amiri R, Barifcanci A. Design and operation of pilot plant for CO<sub>2</sub> capture from IGCC flue gases by combined cryogenic and hydrate method. *Chem Eng Res Des* 2011;89:1752–7.
- [341] Dashti H, Fraser G, Amiri A. Reactor scale modelling of gas hydrate-based CO<sub>2</sub> capture (HBCC) process. *Comput Aided Chem Eng* 2021;50:1073–9. Elsevier.